

Towards a Comprehensive Theory of Metal-Insulator Transitions in Doped Semiconductors

S. Kettemann¹

¹Constructor University (former Jacobs University) Bremen, Bremen 28759, Germany

(Dated: October 5, 2023)

A review is given on the theory of metal-insulator transitions (MIT) in doped semiconductors. We focus in particular on reviewing theories of their anomalous magnetic properties, which emerge from the interplay of spin and charge correlations and disorder. Building on the review of these existing theories and experiments, we suggest that the finite temperature phase diagram can be structured into 1. a quantum spin liquid phase at subcritical doping and low temperature, as described by the Bhatt-Lee theory of random spin clusters, mostly random singlets. 2. a critical non-Fermi-liquid fan, originating at the MIT, which is dominated by random Kondo singlets with a universal tail of the distribution of their binding energies. This is caused by multifractality and results in an anomalous power law divergence of the magnetic susceptibility with a universal power and 3. a supercritical, low temperature phase. Rare events caused by the random placement of dopants do not allow to define strict phase boundaries. Remaining open problems are reviewed and outlined. Finally, the possibility of finite temperature delocalization transitions is reviewed, which are caused by the correlation induced temperature dependence of the spin scattering rate from magnetic moments. This review article is devoted to the memory of Konstantin B. Efetov.

I. INTRODUCTION

Doped semiconductors, such as $\text{Si}_{1-x}\text{P}_x$ (Si:P), are well known to show a metal-insulator transition (MIT) by variation of the dopant concentration x . Although silicon is one of the most intensively studied materials in human history and the MIT in doped silicon has been long known as a paradigm of quantum phase transitions, it remains only partially understood¹⁻⁴. While the doping increases the charge carrier density and thereby the overlap integral between dopant wave functions, the random positioning of the dopants results in random hopping amplitudes between dopant sites. Randomness causes the charge carriers to remain localized below a critical dopant density⁵, the celebrated Anderson localization. However, there are indications of strong spin and charge correlations at low dopant densities and in the vicinity of the MIT, where the electron-electron interaction is poorly screened, giving rise to anomalous magnetic, transport and optical properties. Therefore, while the transition to a metal in doped semiconductors is found to be very similar to an Anderson MIT (AMIT)⁵, driven by disorder, rather than a correlation-driven Mott transition⁶, there is experimental evidence for non-Fermi liquid behavior due to the presence of local magnetic moments (MMs). Thus, a theory of the MIT in doped semiconductors as function of dopant concentration or pressure requires to fully model both disorder^{5,7-13}, and spin and charge correlations^{3,6,7,9,14-21}.

This makes the derivation of its critical properties one of the most demanding challenges in condensed matter theory^{7-9,12}. Getting a more complete understanding of the MIT in one of the best studied materials, silicon, will improve the understanding of the MIT in other, more complex materials, such as SrTiO_3 ²² or the cuprates²³⁻²⁷ and will be of crucial relevance for understanding the

doping dependence in topological insulators²⁸, topological superconductors²⁹, and the superconductor-insulator transition in doped semiconductors^{22,30}. Moreover a better understanding of the interplay of disorder and spin and charge correlations in doped semiconductors may improve their design as functional materials, such as dilute magnetic semiconductors³¹, high efficiency solar cell concepts, like intermediate band solar cells³²⁻³⁴ or dye sensitized solar cells³⁵ and thermoelectric devices³⁶⁻³⁸.

II. SCALING THEORY

The MIT in doped semiconductors is consistent with a second order quantum phase transition where the localization length and correlation length diverge, on the respective sides of the transition³⁹⁻⁴¹, even though the possibility of a discontinuous transition with a minimum metallic conductivity⁴² is also considered⁴³. Measurements of conductivity are found to be consistent with Wegner scaling¹³ with dopant density N at finite temperature T , $\sigma(N, T) = \xi(N)^{2-d} f[T/\Delta_\xi]$, where $f[x]$ is a scaling function. This yields with the correlation length $\xi(N) \sim |N - N_c|^{-\nu}$ with the critical dopant density N_c and the corresponding energy scale $\Delta_\xi \sim \xi(N)^{-z}$, where z is the dynamical exponent, for dimension $d = 3$

$$\sigma(N, T) = \left(\frac{|N - N_c|}{N_c} \right)^\mu F\left[T \left(\frac{|N - N_c|}{N_c} \right)^{-z\nu} \right], \quad (1)$$

where $F[x]$ is a scaling function. It follows that at criticality the conductivity scales with temperature as $\sigma(N_c, T) = \sigma_c(T) \sim T^{\mu/(z\nu)}$. Wegner scaling corresponds to $\mu = \nu$, but in fitting the experiments μ is often allowed to be an independent parameter⁴⁰. For the Anderson transition of noninteracting disordered electrons, Δ_ξ is on the insulating side of the transition the local level

spacing, so that $z = d$ and $\mu = \nu$. It should be noted that the one parameter scaling of the conductivity Eq. (1) is only justified, if the localisation length is self averaging, that is, if it has a normal distribution, which has been confirmed for the Anderson localisation transition numerically, for a review see Ref.⁸.

The scaling of conductivity of uncompensated bulk ($d = 3$) Si:P was done in Ref.³⁹, where the authors assumed $\mu = \nu$ and found $z \approx 2.4$ and $\nu \approx 1.3$. In Ref.⁴⁰ the MIT in Si:B was studied as function of stress. They find $\mu \approx 1.6$ and $z\nu \approx 3.2$. Assuming $\mu = \nu$, this yields thus $\nu \approx 1.6$ and $z \approx 2$. In Ref.⁴¹ the MIT in p-doped uncompensated semiconductor, Ge:Ga has been studied as function of doping concentration. They find $\mu = \nu \approx 1.2$ for $z \approx 3$. For compensated Ge:Ga,As, they rather find $\mu = \nu \approx 1$ for $z \approx 3$. Earlier measurements gave $\nu \approx 1$ ^{8,44}.

The scaling theory of the Anderson transition was conjectured in Ref.⁴⁵ in terms of the flow of the dimensionless conductance g with system size L , building on Refs.^{13,46}. Wegner formulated that scaling theory in a field-theoretical description in terms of the nonlinear sigma model⁴⁷. This effective model for the long wave length physics, which captures in particular diffusion modes originating from multiple impurity scattering was then derived for disordered electron systems, performing the disorder averaging nonperturbatively with the Replica trick in Refs.⁴⁸⁻⁵⁰ and with the supersymmetry method by Efetov¹⁰, both without and with magnetic field and in the presence of spin-orbit coupling and magnetic impurities. A resummation of singularities in perturbation theory provided further evidence of Anderson localisation in $d \leq 2$ dimensions without magnetic field^{51,52}. The Anderson transition was studied in $d = 2 + \epsilon$ expansion of the nonlinear sigma model upto 4-loop order^{53,54} and 5-loop order⁵⁵, on the Bethe lattice⁵⁶⁻⁵⁹ and in effective medium approximation⁶⁰ and⁶¹, yielding in $d = 3$ estimates for the critical exponent $\nu \approx 1$. Recently the conformal bootstrap method has been applied to the Anderson transition in 2D with spin-orbit interaction, and suggested to be a way to get more accurate estimates for the critical exponent ν also for the 3D Anderson transition⁶².

Numerical transfer matrix calculations for the 3D Anderson tight binding (Atb) model of noninteracting disordered fermions⁸ gave for the critical exponent without magnetic field $\nu = 1.571 \pm .004$ ⁶³ and finite size scaling of the distribution of wave function intensities yields $\nu = 1.59 \pm .006$ ⁶⁴.

The discrepancy with the experimental results could be due to interaction effects. Local interactions can create magnetic moments in weakly coupled impurity sites⁶⁵⁻⁶⁷. In Ref.⁶⁸ the 3D Atb model of noninteracting disordered fermions with hopping amplitude t was studied when the electron spin is coupled by exchange coupling J to a finite concentration of classical magnetic moments. The critical exponent was found for $J > 0.3t$, to be $\nu_S \approx 1.3 \pm 0.1$ when 5 percent of all lattice sites have

magnetic moments⁶⁸, which is in fair agreement with experiments on uncompensated bulk ($d = 3$) Si:P³⁹.

A density functional theory analysis of a model of randomly distributed donor impurities with long range Coulomb interactions between spinless charge carriers yields $\nu = 1.30(+0.12, -0.06)$ ⁶⁹, which is also in good agreement with experimental results³⁹, as well.

A self consistent Hartree Fock treatment of disordered electrons with long range interactions yields a smaller ν , which is found to depend on the interaction range⁷⁰ and for the diverging correlation length a different ν_M was obtained than for the diverging localization length ν_I on the insulator side of the MIT.

A typical medium dynamical cluster approximation for disordered electronic systems has been applied to the disordered Anderson-Hubbard model, a model with onsite interactions, identifying the mobility edge and the finite temperature phase diagram⁷¹. Parameter-free ab-initio calculations of doped Si:P which employed density functional theory to build a tight binding model, that is then diagonalised numerically, have been used to address the exponent puzzle for the Anderson transition in both compensated and uncompensated doped semiconductors in Ref.⁷².

Cold atom experiments on the Anderson localization transition in $d = 3$ reported critical exponents $\nu \approx 1.6$ ^{73,74}. In these systems interactions are known to be weak, which explains the good agreement with the results of the noninteracting tight binding model^{63,64}.

The many-body theory of the MIT in doped semiconductors has a long history. It is well established^{7,9} that long range Coulomb interactions in strongly disordered metals give rise to Althshuler-Aronov corrections to the density of states (DOS) and to the temperature dependence of the conductivity on the metallic side of the MIT. In 3D it gives $\sigma \sim \sigma_0 - \sigma_0^2 A T^{1/2}$, where σ_0 is the residual conductivity and A an interaction dependent constant. This corresponds according to Eq. (1) for $\mu = \nu$ to a dynamical exponent $z = 2$ ⁷⁵⁻⁷⁷. For a review see Ref.⁷⁸. This is in strong contrast to the Fermi liquid conductivity of a pure metal, where the electron-electron scattering rate is proportional to T^2 , which would rather yield $z = 1/2$. On the insulator side of the MIT Coulomb interactions give rise to the Coulomb gap in the DOS. Transport of electrons can be modeled there by Efros-Shklovskii variable range hopping conductivity⁷⁹, which is consistent with Wegner scaling for $N < N_c$, when $\sigma(N, T) = \sigma_c(T) \exp(-(\Delta_\xi(N)/T)^p)$, where $\Delta_\xi(N) \sim (N_c - N)^{z'\nu}$. Here, the dynamical exponent z' should, for consistency, be equal to z . In fitting experiments it is sometimes taken as an independent fitting parameter. Here, $p = 1/2$ or $p = 1/4$ depending on the dominant hopping process⁷⁹.

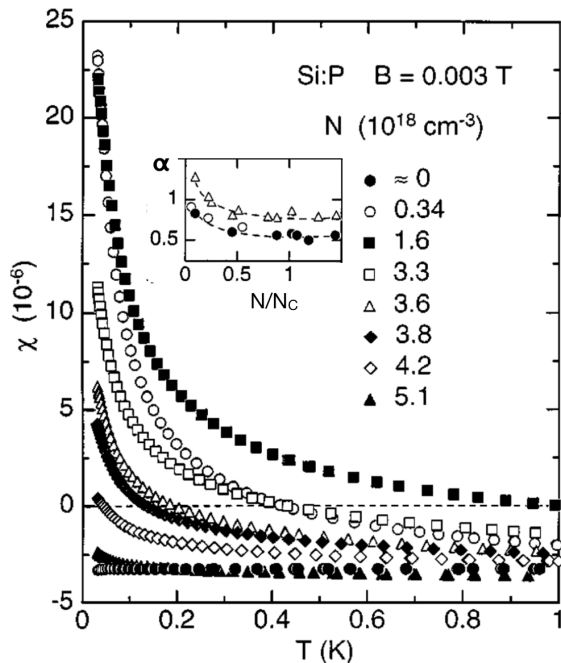


FIG. 1. Measured magnetic susceptibility for various doping concentrations N ⁸⁴. Inset: Power α , as obtained by fitting $\chi(T) \sim T^{-\alpha}$ (circles), and by fitting the magnetic moment contribution to the specific heat to $C(T) \sim T^{1-\alpha}$ (triangles), plotted as function of N/N_c . Figs. taken and reedited from Ref.⁸⁴, Copyright 1997 Institute of Physics Science.

III. ANOMALOUS MAGNETIC PROPERTIES

A. Experiments

Magnetic susceptibility and specific heat measurements of doped semiconductors like Si:P^{3,17,20,80-84} as well as ESR measurements⁸⁵ provide evidence for magnetic moments (MMs). The magnetic susceptibility is experimentally found to diverge at low temperature with a power law $\chi \sim T^{-\alpha}$, see Fig. 1. The fitted power α is plotted as function of dopant density N in the inset of Fig. 1 (circles), while an analysis of the contribution of MMs to the specific heat measurements yields $\alpha(N)$ in the inset of Fig. 1 (triangles)^{3,84}. In the dilute limit $N \leq 1/a_B^3$, where a_B is the Bohr radius of the dopants, the magnetic susceptibility is observed to follow the Curie law $\chi \sim N/T$. This is in agreement with the fact that in Si:P all dopants have a free $S = 1/2$ -spin, only weakly coupled by the antiferromagnetic super-exchange interaction between the hydrogen like dopant levels¹⁴. For increasing doping concentration N , the power α is found to decrease continuously. Close to the transition $N_c = 3.3 \times 10^{18}/\text{cm}^3$, the power converges to $\alpha \approx .5$, and hardly depends on N deep into the metallic phase. At the same time, the amplitude of the magnetic susceptibility decays with increasing concentration N , indicating a decrease of the concentration

of MMs $n_M < N$.

At the MIT $N = N_c$ and in the metal regime $N > N_c$ a finite concentration of spin- $1/2$ MMs have been shown to be created by the onsite interaction in weakly coupled impurity sites⁶⁵⁻⁶⁷, positioned randomly and coupled weakly by antiferromagnetic super-exchange interactions^{3,6,16}. The concentration of MMs decreases with increasing doping. At the MIT theoretical calculations^{66,86} and the evaluation of experiments³ are consistent with about 10 % of all dopants forming MMs. In Ref.⁸⁷ it was pointed out that a combined analysis of magnetic susceptibility and electron spin resonance experiments gives hints that at least part of the low temperature enhancement of the magnetic susceptibility could be rather due to an anomalous intensification of the interaction between electrons by disorder.

In a metal the exchange coupling J of spin $1/2$ -MMs to the conduction electrons results below a temperature scale T_K in the screening of the MM by a cloud of conduction electron spins, the Kondo effect⁸⁸⁻⁹². Above the Kondo temperature T_K the MMs contributes a Curie like term to the magnetic susceptibility. At temperatures below T_K the contribution to the susceptibility converges to a temperature independent Pauli like contribution since the MMs become screened. Nagaoka⁸⁹ and Suhl⁹⁰ derived for a non-disordered metal with a density of states ρ at the Fermi energy ε_F the Kondo temperature T_K as $T_K^0 \approx c \varepsilon_F \exp(-1/(\rho J))$, where $c \approx 1.14$. The temperature dependence of thermodynamic observables like the magnetic susceptibility and transport properties obey in a clean metal universal scaling functions, which scale with T_K .

Indeed, the Kondo effect has been detected experimentally in doped semiconductors for $N > N_c$ by thermopower measurements which, when fitting with the theory of Ref.⁹³, is consistent with a Kondo temperature $T_K \approx 0.8\text{K}$ ⁹⁴. Therefore, it is experimentally evident that the Kondo effect has to be taken into account in the theory of the anomalous magnetic properties of doped semiconductors in the vicinity of the MIT.

While the Kondo problem has been previously solved in clean metals⁸⁸⁻⁹¹, a comprehensive theory of the MIT requires to consider the Kondo impurities coupled to the strongly disordered electron systems in the vicinity of the MIT in doped semiconductors.

B. Distribution of the Kondo temperature

Since the Kondo temperature in a clean metal⁸⁸⁻⁹⁰ depends on the product of the local exchange coupling J and the density of states at the Fermi energy ρ , it is natural to expect a distribution of the Kondo temperature, $P(T_K)$, when J and ρ are distributed due to the random placement of the dopants. Early theories derived thereby $P(T_K)$ from the distribution of J , assuming that the dopants are on random, uncorrelated lattice sites^{19,95}, finding a magnetic susceptibility with correc-

tions to the Curie law, $\chi(T) \sim \exp(-kNa^3 \ln^3(T_0/T))/T$, where k is a constant, $T_0 \sim Zt$, where Z is the average degree of the random network of dopants, and t the average hybridisation energy between neighbored dopant sites (for Si:P $t \approx 28\text{meV}$ was estimated in Ref.⁹⁵). Inserting the local density of states $\rho(\epsilon, x)$ which is known to have a wide, lognormal distribution at the AMIT into $T_K \sim \exp(-1/(\rho J))$, $P(T_K)$, was derived in Ref.⁹⁶, and shown to yield also weak corrections to the Curie law for the magnetic susceptibility^{96, 21}.

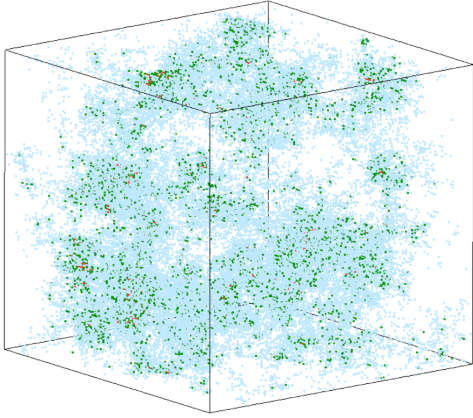


FIG. 2. Intensity of critical state of the 3D Atb model (disorder amplitude $W = 16.5t$, t hopping parameter, at energy $E = 2t$, size $L = 100a$, lattice spacing a). Coloring denotes $\alpha_\psi = -\ln|\psi|^2/\ln L \in [1.2, 1.8], [1.8, 2.4], [2.4, 3.0]$, (red, green, light blue), respectively. Fig. taken from Ref.¹⁰³, Copyright 2012, American Physical Society.

The influence of the disorder in the electron system on the Kondo effect is more subtle, however. In 1-loop approximation, the Kondo temperature at site \mathbf{r} of a spin-

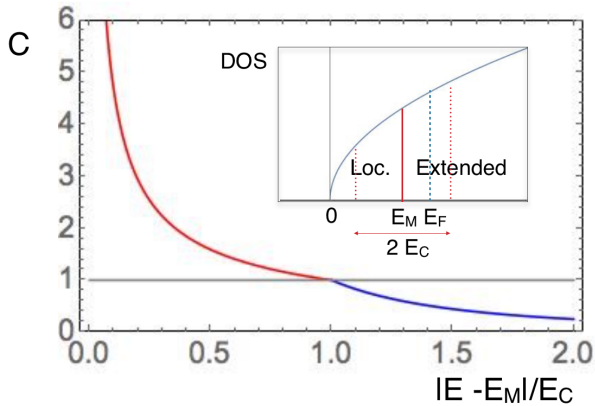


FIG. 3. Correlation function of intensities, C , as function of energy difference $|E - E_M|$ in 3D disordered system, $\eta \approx 2$. Inset: Density of states as function of E . Intensities are correlated within energy E_c around mobility edge E_M . Fig. taken from Ref.¹⁰⁴, Copyright 2016, American Physical Society.

1/2-impurity is determined by^{89,90}

$$1 = \frac{J}{2N_L} \sum_{n=1}^{N_L} \frac{L^d |\psi_n(\mathbf{r})|^2}{E_n - E_F} \tanh\left(\frac{E_n - E_F}{2T_K}(\mathbf{r})\right), \quad (2)$$

where N_L is the total number of energy levels in a finite sample of linear size L , $|\psi_n(\mathbf{r})|^2$ is the probability density of the eigenstate at the site \mathbf{r} of the spin-1/2-impurity. In a clean metal the Eigenstates are plane waves with uniform intensity $|\psi_n(\mathbf{r})|^2 = 1/L^d$, The disorder results in wavefunction amplitudes which vary with the position \mathbf{r} . In a weakly disordered metal different wave functions are correlated with each other in a macroscopic energy interval of the order of the elastic scattering rate $1/\tau$. Thus, in a weakly disordered metal the Kondo temperature is found to have a finite width in the thermodynamic limit⁹⁷⁻⁹⁹.

However, at the AMIT the wave functions are strongly inhomogenous and multifractal¹⁰⁰ with power law correlations in energy^{101,102}. Since the AMIT is a 2nd order quantum phase transition the localization length ξ and the correlation length ξ_c diverge at the AMIT. Thus, the electrons at the AMIT are in a critical state, which is neither extended nor localized. In fact it is rather sparse, see Fig. 2, where the intensity $|\psi_n(\mathbf{r})|^2$ is plotted for all sites of a finite sample of the 3D Atb model. At the AMIT the q -th moment of eigenfunction intensities $|\psi_l(\mathbf{r})|^2$ is found to scale with linear size L as

$$P_q = L^d \langle |\psi_l(\mathbf{r})|^{2q} \rangle \sim L^{-d_q(q-1)}. \quad (3)$$

Critical states are characterized by multifractal dimensions $d_q < d$ which change with power q . The resulting distribution function of the intensity is for the 3D AMIT very close to a log-normal distribution function^{12,64}

$$P(|\psi_l(\mathbf{r})|^2) \sim \frac{1}{|\psi_l(\mathbf{r})|^2} L^{-\frac{(\alpha_\psi - \alpha_0)^2}{2\eta}}. \quad (4)$$

Here, $\alpha_\psi = -\ln|\psi_l(\mathbf{r})|^2/\ln L$, $\eta = 2(\alpha_0 - d)$ and $\alpha_0 > d$. The multifractal dimension d_q is related to α_0 by $d_q = d - q(\alpha_0 - d)$ for $q < q_c$. At $q_c = \alpha_0/\eta$ the function $\tau_q = d_q(q-1)$ terminates at τ_{q_c} and does not change for larger moments, $q > q_c$ ¹². Approaching the AMIT, single particle wave functions show multifractality when looking at length scales which are smaller than ξ , ξ_c , respectively¹⁰⁰. Another consequence of multifractality is that the intensities are power law correlated in energy^{101,102,105}, see Fig. 3 and in space¹². The correlation function of intensities associated to two energy levels is found to decay with a power law of their difference $\omega_{nm} = E_n - E_m$ as^{102,105}

$$C(\omega_{nm} = E_n - E_m) = L^d \int d^d r \langle |\psi_n(\mathbf{r})|^2 |\psi_m(\mathbf{r})|^2 \rangle = \begin{cases} \left(\frac{E_c}{\text{Max}(|\omega_{nm}|, \Delta)}\right)^{\eta/d}, & 0 < |\omega_{nm}| < E_c, \\ \left(\frac{E_c}{|\omega_{nm}|}\right)^2, & |\omega_{nm}| > E_c, \end{cases}, \quad (5)$$

when $E_n \leq E_M$ and $E_m \geq E_M$ or the other way around, as plotted in Fig. 3. $\Delta = 1/(\rho L^d)$ is the average level

spacing, ρ the average density of states. Here, we set one of the energies at the mobility edge $E_n = E_M$ and the other at $E_m = E$. The correlation energy E_c is found to be of the order of elastic scattering rate $1/\tau$. For $|\omega_{nm}| < E_c$ correlations are enhanced compared to the plane wave limit $C_{nm} = 1$, see Fig. 3. Recently, it was shown in numerical simulations^{69,70,106} and using the nonlinear sigma model of disordered interacting fermions^{107,108} that multifractality persists in strongly interacting disordered fermion systems with *long range interactions*. In cases when the interacting states cannot be written as Slater determinants of single particle states, one can formulate the problem in terms of local density of states (LDOS). In Ref.¹⁰⁸ the LDOS at the MIT was studied and confirmed to have a multifractal distribution.

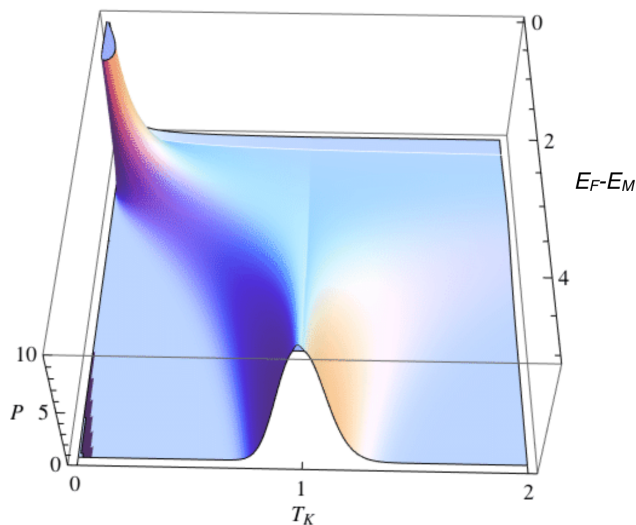


FIG. 4. Distribution of Kondo temperatures T_K in units of $T_K^{(0)}$ in the metallic phase, acc. to analytical theory Eq. (25) of Ref.¹⁰³, as function of distance to mobility edge $E_F - E_M$ in units of E_c for exchange coupling $J = D_0/5$, D_0 band width. Fig. taken from Ref.¹⁰³, Copyright 2012, American Physical Society.

Implementing these power law correlations of local wavefunction intensities, an analytical result for the distribution of T_K at and in the vicinity of the AMIT has been obtained in Ref.¹⁰³, using that the distribution of wave function intensities is close to log-normal. That distribution of T_K is found to widen as the system approaches the AMIT from the metallic side, evolving into a distribution with a power law divergent low T_K -tail. That tail has been shown in Ref.¹⁰³ to originate from the opening of local pseudo gaps, which quench the Kondo screening. The full distribution of T_K , Eq. (25) of Ref.¹⁰³, is plotted in Fig. 4 as function of the distance to mobility gap E_M , approaching it from the metallic side. At the mobility gap $E = E_M$ its tail is found to be given

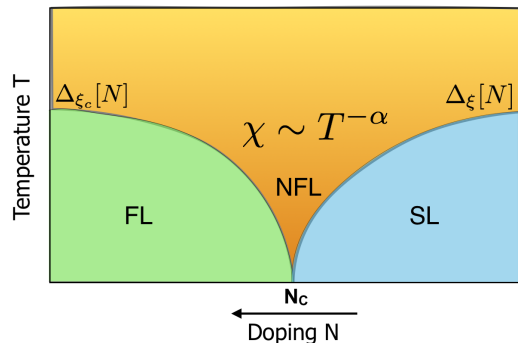


FIG. 5. Schematic phase diagram as function of doping concentration N and temperature T . Anomalous magnetic susceptibility $\chi \sim T^{-\alpha}$ with universal power $\alpha = 1 - (\alpha_0 - 3)/3$ at criticality N_c and for $T > \Delta_\xi$ in the insulator regime $N < N_c$, and for $T > \Delta_{\xi_c}$ in the metal regime $N > N_c$.

by

$$P(0 < T_K \ll T_K^0) \sim T_K^{-\alpha}, \quad (6)$$

with power $\alpha = 1 - \eta/(2d)$, depending only on the multifractal correlation exponent $\eta = 2(\alpha_0 - d)$. In the vicinity of the AMIT that universal power law tail remains valid on the metallic side $N > N_c$ for $T_K > \Delta_\xi$, and on the insulating side $N < N_c$ for $T_K > \Delta_\xi$, where only at lower temperatures the Kondo screening is fully quenched by local gaps Δ_ξ and a finite density of free magnetic moments remain. This analytical result for the distribution function of T_K allows to calculate the magnetic susceptibility noting that $\chi(T) \sim n_{FM}(T)/T$ with $n_{FM}(T) = n_M \int_0^T dT_K P(T_K)$, yielding¹⁰³,

$$\chi(T) \sim \left(\frac{T}{E_c}\right)^{-\alpha}, \quad (7)$$

valid at the MIT $N = N_c$, on the insulating side $N < N_c$ for $T > \Delta_\xi$ and on the metallic side $N > N_c$ of the MIT for $T > \Delta_{\xi_c}$. This results in the fan like phase diagram, shown schematically in Fig. 5. The contribution of MMs to the specific heat is obtained from $C(T) \sim T dn_{FM}(T)/dT$ as $C(T) \sim T^{\eta/(2d)}$. In $d = 3$ we thus find that the anomalous power of the magnetic susceptibility α has a universal value, independent of doping concentration N , as given by

$$\alpha = 1 - (\alpha_0 - 3)/3, \quad (8)$$

in the vicinity of the MIT. The multifractal parameter α_0 is without magnetic field known numerically to be $\alpha_0 = 4.048(4.045, 4.050)$ ⁶⁴, yielding $\alpha = .651(.652, .650)$. Thus, the critical power law tail of the distribution of the Kondo temperature results in an anomalous power for the temperature dependence of the magnetic susceptibility which is in good agreement with experiments in the vicinity of the MIT, see the inset (circles) of Fig. 1

of Ref.⁸⁴ and results reported in Ref.⁶⁷. If this interpretation is correct, it would make these experiments the first, albeit indirect, measurements of multifractality at the MIT in doped semiconductors.

A direct numerical calculation of the distribution of the Kondo temperature, by application of the Kernel polynomial method¹⁰⁹ to Eq. (2) was reported in Ref.¹¹⁰. In the Atb model with $D = 12t$ in $d = 3$ at the AMIT for $J = 4t$ a low T_K divergence corresponding to the anomalous power of the magnetic susceptibility of $\alpha \approx 0.75$ was found¹¹⁰. This value is very close to the one obtained by numerical exact diagonalisation at the AMIT of the three dimensional Atb in Ref.¹¹¹. The remaining discrepancy with the analytical value can be attributed to the two main approximations employed in the analytical derivation: 1. parabolicity of the multifractal spectrum $f(\alpha)$, and 2. taking into account only pair correlations between electronic intensities at different energies. The multifractality parameter α_0 was found numerically to change in presence of MMs for the $d = 3$ Atb model to $\alpha_0 = 4.53 \pm .07$ ⁶⁸. Inserting this value into Eq. (8) yields for the anomalous power of the magnetic susceptibility $\alpha = .49 \pm .02$, improving the agreement with the measured values, given in the inset of Fig. 1, further.

Going beyond the 1-loop equation for the Kondo temperature, Eq. (2), it was found in Ref.¹¹² that the distribution obtained by a full Wilson renormalization group (RG) calculation^{91,92} for a disordered system yields a qualitatively similar distribution function. Recently, it was pointed out that a more realistic model of the Kondo impurity which takes into account anisotropies may yield a modified distribution of Kondo temperature¹¹³. It remains to be explored whether this will affect the low T_K tail at the AMIT and thereby the anomalous power of the magnetic susceptibility α .

IV. COUPLING BETWEEN MAGNETIC MOMENTS, SPIN LIQUIDS

Even though there is thus convincing evidence that the distribution of Kondo temperature is dominating anomalous magnetic properties close to the MIT in doped semiconductors, for uncompensated Si:P in a temperature range of $10\text{mK} < T < 1\text{K}$ with an average Kondo temperature of about $\langle T_K \rangle \approx 0.8\text{K}$ ⁹⁴, there is also evidence that there remains a finite density of free MMs on the insulating side of the transition in the low temperature limit, since the Kondo screening becomes quenched by Anderson localisation, where the renormalisation of the Kondo coupling becomes cutoff by the local level spacing $\Delta_\xi = 1/(\rho\xi^3)$ ¹¹⁴. Therefore, at temperatures $T < \Delta_\xi$, see Fig. 5, a finite density of free MMs remains which in the zero temperature limit is found to be given by $n_{\text{FM}}(T = 0\text{K}) = n_M \xi^{-\frac{1}{2n}(dj)^2}$ ¹⁰³. In a system of finite linear size L it is found that at the AMIT the concentration remains finite, given by $n_{\text{FM}}(T = 0\text{K}) = n_M L^{-\frac{1}{2n}(dj)^2}$, vanishing only in the thermodynamic limit.

The numerical finite size calculations in Ref.¹¹⁰ found even a much larger concentration of free MMs at the AMIT. In Ref.¹⁹ it was found that even on the metallic side of the MIT there can remain free MMs due to rare sites which due to the random placement of dopant sites remain strongly isolated.

A. Random Singlet State

Since these MMs are still weakly coupled to the electron system, which mediate the exchange coupling, the MMs are coupled with each other. In the dilute limit it is the super-exchange coupling as derived from the overlap of hydrogen like impurity states between neighbored dopants, which is known to be antiferromagnetic. The randomly positioned MMs have therefore been modeled by a Heisenberg spin model with random antiferromagnetic short range, exponentially decaying super-exchange interaction¹⁴⁻¹⁸. In agreement with experiments, numerical simulations and the implementation of a cluster renormalisation group by Bhatt and Lee for this model have found no evidence of a spin glass transition, at which the magnetic susceptibility would peak and then decay to lower temperatures^{15,16}. Rather, the magnetic susceptibility of that model diverges at low temperature with a power law $\chi(T) \sim T^{-\alpha}$, with $\alpha \leq 1$ ^{15,16}. In one dimension, the random antiferromagnetic short range Heisenberg model is known to flow at low temperature to the infinite randomness fixed point, where the ground state is formed of randomly placed spin singlets, the so called *random singlet phase*. This can be derived by the strong disorder RG (SDRG) method. The temperature dependence of its magnetic susceptibility is found to diverge almost Curie like^{15,16}, and can be derived analytically in 1D, yielding only logarithmic corrections to the Curie law as $\chi(T) \sim T^{-1}/\ln^2(\Omega_0/T)$ ¹¹⁵.

B. Large Spin Fixed Point

When the localisation length ξ exceeds the Fermi wave length λ_F , however, the interaction between spins is longer ranged and oscillates in sign with distance, similar to the RKKY interaction in the metallic regime¹¹⁶, but decaying exponentially beyond the localisation length ξ . A short-range Heisenberg model with random sign coupling was studied using a modified version of the SDRG method in Refs.^{117,118}: If the strongest bond is AF it forms a singlet and adjacent spins are coupled by renormalized interactions. If the strongest bond is FM the Hamiltonian is rather projected onto triplet states with reduced couplings. For chains it was thereby shown that for any finite number of FM couplings the chain is driven to a new fixed point with clusters forming large effective spins, contributing a Curie law magnetic susceptibility^{118,119}. In higher dimensions it is known that even if the initial distribution is purely antiferro-

magnetic, ferromagnetic couplings can be generated upon renormalization^{16,120}.

Thus, the low temperature magnetic properties of doped semiconductors is expected to be dominated by random singlets in the dilute limit, while at larger doping on the insulating side of the transition, clusters of larger effective spins may form. In both cases, only small corrections to the Curie law are expected in the low temperature limit, where the MMs form a spin liquid, and no spin glass formation is expected, as indicated in the phase diagram Fig. 5.

On the metallic side of the MIT the Kondo screening of the MMs competes with long range indirect exchange interactions. For a pure metal these are known as RKKY interactions¹¹⁶. Close to the AMIT their amplitude is however widely distributed with a lognormal distribution¹²¹, as can be understood as follows. Writing the indirect exchange coupling between MMs in terms of local wave functions $\psi_n(\mathbf{r}_i)$ one gets

$$J_{\text{RKKY}}(\mathbf{r}_{kl}) = \frac{S(S+1)J_{ik}J_{jl}V_0^2}{4\pi S^2} \times \Im \int_{-\infty}^{E_F} d\omega \sum_{n,l} \frac{\psi_n^*(\mathbf{r}_i)\psi_n(\mathbf{r}_j)}{\omega - E_n + i\epsilon} \frac{\psi_l(\mathbf{r}_i)\psi_l^*(\mathbf{r}_j)}{\omega - E_l + i\epsilon}, \quad (9)$$

where $V_0 = L^3/N$. We see, that it depends not only on intensities $|\psi_n(\mathbf{r}_i)|^2$, but also on the phase of the Eigenfunctions. This complicates its evaluation, especially at the MIT. In a clean metal the RKKY-expression is recovered when inserting plane-wave states $\psi_n(\mathbf{r}_i) \sim \exp(i\mathbf{k}\mathbf{r}_i)$ into Eq. (9). This gives for $k_F r_{ij} \gg 1$, $J_{\text{RKKY}}^0(\mathbf{r}_{kl}) \sim J_{ik}J_{jl} \cos(2k_F r_{kl})r_{kl}^{-3}$. Disorder shifts the phases of wave functions randomly. This results in exponential suppression of the couplings, giving $\langle J_{\text{RKKY}} \rangle \sim \exp(-r_{kl}/l_e)$ when averaged over an ensemble of disordered systems, where l_e is the elastic mean free path¹²². The typical value $\sqrt{\langle (J_{\text{RKKY}})^2 \rangle}$ is however found to remain close to J_{RKKY}^0 for weak disorder. At strong disorder and at the AMIT the electron intensities $|\psi_n(\mathbf{r}_i)|^2$ have a lognormal distribution, as reviewed above. Thus, since Eq. (9) is proportional to the intensities at two positions, one arrives at a lognormal distribution of $J_{\text{RKKY}}(\mathbf{r}_{kl})$ ¹²¹. This was confirmed numerically for a 2D disordered system and for graphene in Ref.¹²³.

C. Strong Disorder Fixed Point

Random quantum spin systems with long range exchange interactions have recently been studied by extending the strong disorder RG method to long range coupled transverse Ising chains¹²⁴ and to the random long range coupled antiferromagnetic XX-quantum spin chain¹²⁵⁻¹²⁹. Comparison with numerical exact diagonalization and tensor network extensions of the Density Matrix RG method^{127,129} confirmed that for power law interactions decaying with distance R between the spins as $R^{-\beta}$ these models flow to a strong disorder fixed point,

a random singlet state. The fixed point distribution of the exchange couplings has a finite width $W = 2\beta$ and the power law divergence of the magnetic susceptibility is found to depend on β as $\chi(T) \sim T^{1/\beta-1}$ for $\beta > 1$ ^{126,127}. At $\beta = 1$ there is a delocalization transition and $\chi(T)$ is expected to diverge logarithmically, only.

D. SYK-model

The random sign coupling was taken into account in an SU(M)-model with infinite range interaction whose amplitude is normally distributed^{130,131}, which is related to the SYK-model¹³²⁻¹³⁵. Due to its infinite range interaction, nonperturbative results can be obtained. Performing the disorder average by means of the replica trick¹³⁶ or the supersymmetry method¹³⁷ it can be mapped on a zero-dimensional nonlinear sigma model. For large $M \gg 1$ its ground state was shown to be a spin liquid and the magnetic susceptibility was found to have a logarithmic divergency $\chi(T) \sim |\ln T|^{130,131}$, similar to what had been conjectured for the magnetic susceptibility in marginal Fermi liquids¹³⁸. For spin $S = 1/2$, corresponding to $M = 2$, the ground state was recently found to show spin glass type correlations¹³⁹, similar to the corresponding random classical Ising model with infinite range interaction^{140,141}, but excited states were found in Ref.¹³⁹ to show spin liquid behavior.

E. More Realistic Models of Randomly Coupled Quantum Spins

To get a better understanding of the magnetic properties of doped semiconductors at their MIT, power law long range coupled Heisenberg spin $S = 1/2$ -models with random sign and wide, lognormal distribution of their exchange couplings still need to be studied in $d = 3$. Such studies have been mentioned in Ref.¹⁶ where no spin glass ordering has been found for power law couplings with power $\beta \geq 3$.

Recently, it became possible to explore disordered spin ensembles at a diamond surface by probing it with single nitrogen-vacancy (NV) centers in diamond^{142,143}. Recent advances in experimental setups in cold atom systems allow the study of long range coupled spin systems with interactions that fall-off as $1/r^3$, which has been demonstrated by coupling Rydberg states with opposite parity¹⁴⁴⁻¹⁴⁶. Trapped ions with power-law interactions, decaying as $1/r^\alpha$, with tunable $0 < \alpha < 1.5$ have also been realized¹⁴⁷⁻¹⁴⁹, recently. As these setups allow the controlled experimental study of real systems of randomly coupled quantum spins, they may allow analogue simulations of models and promise to contribute to a better understanding of the magnetic properties of doped semiconductors.

V. COMPETITION BETWEEN KONDO EFFECT, INDIRECT EXCHANGE INTERACTION AND DISORDER

A. Doniach Diagram

The indirect exchange interaction of MMs competes with the Kondo effect as the local exchange coupling J and the concentration of MMs $n_M = R^{-d}$ is varied, where R is the average distance between neighbored MMs. This gives rise to a rich quantum phase diagram, the Doniach diagram^{150,151}, where a Kondo screened phase is separated from a phase which is dominated by the indirect exchange interactions. There, below a critical density n_c , the Kondo effect is prevailing the RKKY interaction. For an electron system without nonmagnetic disorder that critical density is found from the condition $|J_{\text{RKKY}}^0(R_c)| = T_K$. For example, in a 3D sample with $|J_{\text{RKKY}}^0|_{k_F R \gg 1} = J^2 \rho(\varepsilon_F) \frac{\cos(2k_F R)}{32k_F^3 R^3}$ and $T_K = c\varepsilon_F \exp(-1/(\rho J))$, where k_F is the Fermi momentum and $c \approx 1.14$, one finds the critical electron density $n_c = 32c \frac{\varepsilon_F}{\rho J^2} \exp(-\frac{1}{\rho J})$, increasing with J in the relevant coupling range $J\rho < 1$. In a disordered system the Kondo temperature T_{K_i} is different at each site \mathbf{r}_i and competes with the RKKY coupling $J_{\text{RKKY}}(\mathbf{R}_{ij})$ with other MMs which are located at sites \mathbf{r}_j at distance \mathbf{R}_{ij} . Their ratio $J_{\text{RKKY}}(\mathbf{R}_{ij})/T_{K_i}$, varies across the disordered sample. This problem has been studied with a disordered Kondo lattice model¹⁵²⁻¹⁵⁴ and with the Anderson-Hubbard model with numerical methods, including dynamical mean field theory based approaches¹⁵⁵⁻¹⁶², and Hatree-Fock based approaches^{86,163,164}, quantum Monte Carlo¹⁶⁵⁻¹⁶⁷, and the typical medium dynamics cluster approximation^{168,169}. In Refs.^{168,169} the quasiparticle self energy of the Anderson-Hubbard model was derived as function of excitation energy ω , $Im\Sigma(\omega) \sim \omega^{\alpha_\Sigma}$. It was found to behave as a non-Fermi liquid with power $\alpha_\Sigma(W) < 2$, which was found to become smaller with stronger disorder amplitude W . The non-FL is found to extend down to the lowest energy at the MIT, while there is a crossover away from the MIT, as limited by a cutoff which coincides with the local level spacing in the insulator phase, $\Delta_\xi = 1/(\rho\xi^d)$, and $\Delta_{\xi_c} = 1/(\rho\xi_c^d)$, in the metal phase, respectively. This is in agreement with the phase diagram derived from the magnetic properties and reviewed above, as shown in Fig. 5. Ref.¹⁶⁸ also reported the distribution of Kondo temperatures, as defined by the width of the spectral function peak, and found that it widens at the MIT into a power law tail, qualitatively very similar to our analytical result, shown in Fig. 4. Since the typical medium dynamics cluster approximation does not model indirect exchange interactions, the Doniach diagram was not studied in Ref.¹⁶⁸.

In order to get a better understanding of the Doniach diagram in disordered systems the distribution of the ratio between $J_{\text{RKKY}}(\mathbf{r}_{ij})$ and T_{K_i} has been calculated in Ref.¹²³, as shown in Fig. 6 a) for a 2D Atb model for

four distances R between two arbitrary MMs. The black dashed arrows highlight a sharp cutoff found for these distributions. In Fig. 6 b) we show the critical MM density $n_c(J)$ (as determined by the distance R_c , which is defined by the condition $|J_{\text{RKKY}}(R)/T_K| < 1$ for all $n_M = 1/R^d < n_c = 1/R_c^d$) as function of exchange coupling J in units of band width D_0 , for three disorder strengths W . At strong disorder, the RKKY coupling is exponentially cutoff by the localisation length, yielding at small densities a local moment phase (LM). While such a study remains to be done in 3D disordered systems at the AMIT, we can deduce from the study in 2D, Fig. 6, that the coupling between MMs becomes more likely to dominate the Kondo screening as the MIT is approached, since the density of MMs and the disorder strength increases as the doping density is reduced towards the MIT.

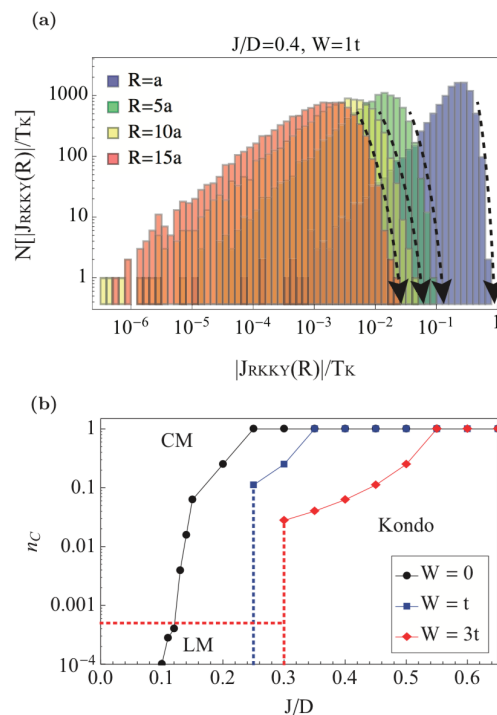


FIG. 6. (a) Distribution of the ratio between $|J_{\text{RKKY}}(R)|$ and T_K for various distances R between two arbitrary MMs for a 2D Tbm. Black dashed arrows highlight the sharp cutoff for each distribution. (b) Magnetic quantum phase diagram: critical MM density n_c (as determined by the distance R_c such $|J_{\text{RKKY}}(R)/T_K| < 1$ for all sites when $n_M = 1/R^d < n_c = 1/R_c^d$) as function of J/D_0 (D_0 is the band width) for various disorder strengths W . Horizontal dashed line separates the local moment phase (LM). Linear system size is $L = 100a$, the number of disorder configurations is 30000.. Fig. taken from Ref.¹²³, Copyright 2014, American Physical Society.

B. Selfconsistent Renormalisation Group Theory of Disordered Kondo Lattices

Including the RKKY coupling between MMs self-consistently in the renormalization group equations for a Kondo lattice¹⁷⁰, it was recently shown that the Kondo temperature decreases when one increases the RKKY coupling. This happens before the Kondo screening is quenched completely at couplings above a critical RKKY coupling. Thus, when considering a disordered system, it is actually not sufficient to calculate $J_{\text{RKKY}}(\mathbf{r}_{ij})$ and T_{K_i} independently, but the effect of $J_{\text{RKKY}}(\mathbf{r}_{ij})$ on T_{K_i} needs to be taken into account. Let us therefore review this theory briefly. The effective Kondo coupling $g_i = \rho_i(\mu)J_i$ of the Kondo impurity at site \mathbf{r}_i with the density of states at the chemical potential per spin $\rho(\mu)$ is governed by RG-equations as modified by the presence of RKKY couplings¹⁷⁰

$$\frac{dg_i}{d \ln D} = -2g_i^2 \left(1 - y_i g_0^2 \frac{D_0}{T_K} \frac{1}{\sqrt{1 + (D/T_K)^2}} \right). \quad (10)$$

D is the energy scale which cuts off the RG-flow. While the first term on the right side is known as the 1-loop β -function of the Kondo effect, the second term takes account of the RKKY coupling. Here, $g_0 = \rho(\mu)J_0$ with bare Kondo interaction J_0 and bare bandwidth D_0 . The effective dimensionless RKKY coupling strength at site \mathbf{r}_i is defined by¹⁷⁰

$$y_i = -\frac{8\mathcal{W}}{\pi^2 \rho(\mu)^2} \text{Im} \sum_{j \neq i} e^{i\mathbf{k}_F \mathbf{r}_{ij}} G_c^R(\mathbf{r}_{ij}, \mu) \Pi(\mathbf{r}_{ij}, \mu) \quad (11)$$

Here, \mathcal{W} is the Wilson ratio, which is known from the Bethe Ansatz solution of the Kondo problem⁹². $G_c^R(\mathbf{r}_{ij})$ is defined to be the conduction band single particle propagator from site \mathbf{r}_i to \mathbf{r}_j . The summation runs over all other MMs at positions \mathbf{r}_j . The RKKY correlation function of conduction electrons between sites \mathbf{r}_i and \mathbf{r}_j is denoted here as $\Pi(\mathbf{r}_{ij}, \mu)$. While the RKKY correlation function oscillates between positive and negative values, y_i is positive¹⁷⁰. We note that the effective Kondo interaction g_i is still a function of D/T_K , even though the RG-equation includes the RKKY-coupling, when T_K is understood to be the renormalized Kondo temperature. T_K has to be found self-consistently from that RG-equation (10).

Considering first two MMs in a clean system, with bare couplings g_0 and $y_i = y$, the solution of the RG-equations gives¹⁷⁰

$$\frac{1}{g} - \frac{1}{g_0} = 2 \ln \left(\frac{D}{D_0} \right) - y g_0^2 \frac{D_0}{T_K} \ln \left(\frac{\sqrt{1 + (D/T_K)^2} - 1}{\sqrt{1 + (D/T_K)^2} + 1} \right). \quad (12)$$

When $D \rightarrow T_K$, one finds that the effective Kondo interaction g diverges, $g \rightarrow \infty$. This condition gives a self-consistent equation for the effective Kondo temperature as a function of the RKKY-coupling,

$$\frac{T_K(y)}{T_K(0)} = \exp \left(- y k g_0^2 \frac{D_0}{T_K(y)} \right). \quad (13)$$

Here, $T_K(0) = D_0 \exp(-1/(2g_0))$ is the bare Kondo temperature without RKKY-coupling and $k = \ln(\sqrt{2} + 1)$. The critical coupling at which the RKKY interaction prevents the Kondo screening completely, is given by¹⁷⁰

$$y_c = T_K^0 / (k e g_0^2 D_0). \quad (14)$$

Recently, this theoretical framework was applied to two MMs with different local density of states at different sites, giving different bare Kondo temperatures, $T_{K_i}^0 = D_0 \exp(-1/(2g_i^0))$ ¹⁷¹. The resulting coupled RG-equations were then solved numerically. Thereby, it was found that both Kondo temperatures are reduced in the presence of the RKKY-coupling. However, the initially smaller Kondo temperature was found to be suppressed more than the initially larger one. Thereby, their ratio $x = T_{K_2}/T_{K_1}$ decreases due to the RKKY-coupling. The smaller the ratio x_0 is, initially, the stronger the inequality x becomes. Thus, inhomogeneity is found to be a relevant perturbation. Any inequality between Kondo temperatures becomes enhanced by the RKKY coupling. Moreover, the Kondo screening is destroyed already by smaller RKKY coupling, the stronger the inhomogeneity and the smaller the initial ratio of bare Kondo temperatures x_0 is. Thus, one can conclude that an inhomogeneity makes the Kondo screening of the magnetic impurities more easily quenchable by RKKY coupling.

For a finite density of randomly distributed MMs, n_M , which are coupled by random local exchange couplings J_i^0 to the conduction electrons with local density of states $\rho(E, \mathbf{r}_i)$ one can extend this approach. Every MM has then, in general, different Kondo temperatures, as they are placed at different positions, yielding a distribution of Kondo temperatures^{6,19,20,103,110,111}. As reviewed above, the RKKY coupling can also have a wide distribution^{19,121,123}. The derivation of the quantum phase diagram of a disordered electron system with finite density of MMs n_M remains therefore an open problem. With the indirect exchange couplings Eq. (11) we can formulate for the coupled, randomly distributed MMs the set of self-consistent RG-equations. Since the local density of states $\rho(\mathbf{r}_i, E)$ does depend on energy E at each RG scale D the renormalisation of local exchange couplings $J(\mathbf{r})$ depends on the local density of states $\rho(\mathbf{r}_i, \mu \pm D)$. Since that can differ strongly from the density of state at chemical potential μ , $\rho_{0i} = \rho(\mathbf{r}_i, \mu)$, it is important to keep this energy dependence. We get for $g_i = J(\mathbf{r}_i)\rho_{0i}$ the RG-equations as

$$\frac{dg_i}{d\ln D} = -g_i^2 \sum_{\alpha=\pm} \left(\frac{\rho(\mu + \alpha D, \mathbf{r}_i)}{\rho_{0i}} - \frac{4J_i^0}{\pi\rho_{0i}} \sum_{j \neq i} J_j^0 \text{Im}[e^{i\mathbf{k}_F \mathbf{r}_{ij}} \chi_c(\mathbf{r}_{ij}, \mu + \alpha D) G_c^R(\mathbf{r}_{ij}, \mu + \alpha D) \chi_f(\mathbf{r}_j, \mu + \alpha D)] \right) \quad (15)$$

While the first term on the right hand side is the well known 1-loop RG for the Kondo problem with energy dependent density of states,^{90,172,173} the second term describes the inhomogenous coupling. Here, $\chi_f(\mathbf{r}_j, E)$ is the f-spin susceptibility of the MM at site \mathbf{r}_j . $G_c^R(\mathbf{r}_{ij}, E)$ is the retarded conduction electron propagator at site \mathbf{r}_i to \mathbf{r}_j . Here, we defined $\mathbf{r}_{ij} = \mathbf{r}_i - \mathbf{r}_j$. $\chi_c(\mathbf{r}_{ij}, E)$ denotes the conduction electron correlation function between sites \mathbf{r}_i and \mathbf{r}_j . Solving Eq. (15) we can thus derive the position dependent Kondo temperatures for a given configuration of indirect exchange interactions.

When the densities of MMs n_M is not too large, $\chi_f(\mathbf{r}_j, E)$ can be approximated by the Bethe-Ansatz solution for a single Kondo impurity⁹². In Ref.¹⁷⁰ this approximation has been used. Then, only its real part contributes, as given by $\text{Re}\chi_f(\mathbf{r}_j, \mu + D) = \mathcal{W}/(\pi T_{Kj} \sqrt{1 + D^2/T_{Kj}^2})$. Here, \mathcal{W} is the Wilson ratio. T_{Kj} is the Kondo temperature of the MM at site \mathbf{r}_j . Since it is well known that the energy dependence of the density of states changes the Kondo renormalisation¹⁷³ and thereby yields a different Kondo temperature function in disordered systems^{99,103,112}, it is important to keep the energy dependence of all functions and not to replace it with their value at the chemical potential.

When knowing the distribution of the local couplings $g_0(\mathbf{r})$ which originates from the random positions of the MMs with random distribution of the local density of states, and the long range function $y(\mathbf{r} - \mathbf{r}')$, we can thus derive the distribution function of Kondo temperatures T_K from Eq. (15). We note that the random distribution of RKKY-couplings is mainly due to the distribution of local couplings $g_0(\mathbf{r})$ ¹²³. Therefore the distribution of T_K comes mainly from local couplings $g_0(\mathbf{r})$, while the function $y(\mathbf{r} - \mathbf{r}')$ is only weakly affected by the disorder.

As reviewed above, without the RKKY-coupling T_K has close to the AMIT a bimodal distribution with one peak close to the Kondo temperature of the clean system and the other peak at low T_K ^{99,103,110,111}. For stronger disorder more weight is shifted to the low T_K peak. At the Anderson MIT it converges to a universal power law tail, as reviewed above, where the power exponent α has a universal value, which depends only on the multifractality parameter α_0 , see Eq. (8)^{103,110}. Since the RKKY-interaction is found to enhance inequalities between Kondo temperatures, it is expected that these interactions shift more weight to the low Kondo temperature peak. This can be checked quantitatively by the solution of Eq. (15).

The interplay of the Kondo effect, indirect exchange interaction and Anderson localization has recently been studied in a 2D experimental setup in a controlled way¹⁷⁴, which may open new research directions towards

a better understanding of this problem.

VI. EFFECT OF MAGNETIC MOMENTS ON THE MIT

Having established the presence of MMs in doped semiconductors across the MIT and deep into the metallic regime, the question arises, how MMs affect the MIT itself. It is well known that Anderson localization is weakened by MMs since their coupling to the spins of itinerant electrons breaks their time-reversal symmetry (TRS) and spin reversal symmetry (SRS)^{10,11,175}, changing the universality class of the AMIT from orthogonal to unitary^{176,177}. The AMIT in 3D disordered systems could accordingly be affected by MMs, decreasing the critical electron density n_c , increasing the critical disorder W_c , and changing the symmetry class of the transition^{176,177}.

A. Scaling Theory of Anderson Localization in an Orbital Magnetic Field

In an external magnetic field in 3D disordered systems this crossover is known to be governed by the parameter $X_B = \xi^2/l_B^2$, with l_B the magnetic length^{175,176}, yielding the scaling Ansatz for the zero-temperature conductivity in a magnetic field, $\sigma(B) = e^2 f(X_B)/(h\xi)$, which thereby becomes a function of the disorder amplitude $W < W_c$ ^{176,177}

$$\sigma(W, B) = (W_c - W)^\nu \tilde{f}(l_B^{-2}(W_c - W)^{-\varphi}) \quad (16)$$

with the scaling function \tilde{f} . This scaling Ansatz implies that the critical disorder $W_c(B)$ (and respectively the critical density $n_c(B)$) depend on magnetic field B ¹⁷⁶. On the other hand, when coming from the metallic side of the transition $W < W_c(B)$, Wegner scaling implies that the zero-temperature conductivity scales in $d = 3$ as $\sigma \sim (W_c(B) - W)^{\nu_B}$, where ν_B is the critical exponent in a magnetic field. Comparison with Eq. (16) thus gives $W_c(B) = W_c + A l_B^{2/\varphi}$, $2/\varphi = 1/\nu$, when $\nu_B \approx \nu$. This scaling of $W_c(B)$ with $\varphi = 2\nu$ has been confirmed with a numerical transfer matrix method in Ref.¹⁷⁸.

B. Two-scale Localization

We note that this scaling with magnetic field B , outlined above, is not the only possibility. A.V. Kolesnikov and K. B. Efetov found in Refs.^{179,180} evidence for 2-scale

localization, where they calculated with the supersymmetry method the impurity averaged spatial density-density correlation function in a disordered wire in a magnetic field, and found two terms decaying exponentially with two different localization lengths, the orthogonal ξ_O (as obtained in disordered wires with TRS) and the unitary one ξ_U (as obtained when the TRS is broken). Thus, they concluded that it is not the localisation length which crosses over with the magnetic field between the orthogonal and unitary limit, but rather the weight of their contribution changes with the magnetic field. Whether this effect is due to two-scale properties of individual wave functions, or rather due to a bimodal distribution function of the localisation length, remains unclear. Numerical calculations which addressed the same problem, albeit considering different properties, did not find indications of 2-scale localization in disordered quantum wires^{181–183}. Other analytical approaches to this problem were either heuristic¹⁸⁴, made assumptions about the scaling with magnetic field¹⁸⁵ or extracted the magnetic field dependence of the localisation length from a different correlation function, the autocorrelation function of spectral determinants¹⁸⁶, which finds a smooth magnetic field dependence of the localisation length in good agreement with experiments¹⁸⁷. Since the supersymmetric calculations given in Refs.^{179,180} for the density correlation functions remain undisputed, and the physical argument in favor of 2-scale localization is plausible, this problem is even more relevant in higher dimensions: In 2D the difference between orthogonal and unitary localisation length is exponentially large^{45,47,48,54,114,188,189} and in 3D the critical disorder differs between the orthogonal and unitary limit. Thus, it is certainly a relevant question to ask, whether the above scaling assumption remains valid in the crossover regime, or whether there is a coexistence of orthogonal and unitary physics. Then, strongly localised states, which do not see sufficient magnetic field and are thus governed by the orthogonal class, could coexist with more extended states, which see sufficient magnetic field to be in the unitary class, resulting in further increase of their localisation length or even their delocalisation. While this review reports in the following results which are based on the scaling of the conductivity with magnetic field, assuming that the localisation length is self averaging with a normal distribution, the question of two scale localisation raised by K. B. Efetov in quasi-1D-wires^{179,180} still needs to be addressed in higher dimensions, and it is in particular a worthwhile problem to study its consequences for the metal-insulator transition in 3D.

C. Scaling Theory of Anderson Localization with Magnetic Moments

Noting that magnetic scattering breaks both TRS and spin symmetry, changing thereby the symmetry class of the transition^{176,177}, that crossover is governed by the

spin scattering rate from MMs τ_s^{-1} through the parameter $X_s = \xi^2/L_s^2$, where $L_s = \sqrt{D_e\tau_s}$ is the spin relaxation length¹⁷⁵, $D_e = v_F^2\tau/3$ the electron diffusion coefficient. When $X_s \geq 1$ the electron spin relaxes before it covers the area limited by correlation length ξ . Thus, the magnetic length l_B becomes in the presence of MMs replaced by the spin relaxation length L_s , yielding for $W < W_c$ the zero-temperature scaling function of the conductivity,

$$\sigma(W, L_s) = (W_c - W)^\nu \tilde{f}(L_s^{-2}(W_c - W)^{-\varphi_s}). \quad (17)$$

However, it was found that φ_s is an anomalous scaling exponent with $\varphi_s \approx 2\nu + 3$, as derived in second-order $d = 2 + \varepsilon$ -expansion within the N-orbital nonlinear sigma model with spin scattering¹⁷⁷. Noting that Wegner scaling of the zero-temperature conductivity in $d = 3$ gives for $W < W_c(L_s)$, $\sigma \sim (W_c(L_s) - W)^{\nu_s}$, where ν_s is the critical exponent with magnetic scattering, we obtain by comparison with Eq. (17) that the critical disorder is shifted to $W_c(L_s) = W_c(0) + W_c(0)AL_s^{-2/\varphi_s}$ when $\nu_s \approx \nu$ and with $\varphi_s \approx 2\nu + 3$. A is a positive constant and $W_c(0)$ is the critical disorder strength without MMs. This relation was confirmed with a numerical analysis in Ref.⁶⁸, where the coupling of conduction electron spins $\vec{\sigma}_i$ to classical spin vectors \vec{S}_i with random orientation was modeled. There, the critical exponent was found to be reduced to $\nu_s = 1.34 \pm 0.01$ for $J/t = 0.45$. Also, the multifractality parameter α_0 was found to change in presence of MMs in $d = 3$ to $\alpha_0 = 4.53 \pm .07$. Inserting this value into Eq. (8) yields for the anomalous power of the magnetic susceptibility the value $\alpha = .49 \pm .02$, in better agreement with the measured values, given in the inset of Fig. 1.

However, the spin scattering rate $\tau_s^{-1}(T)$ from Kondo impurities depends itself on temperature T . At high temperature the MMs with spin S have the magnetic relaxation rate given by $1/\tau_s(T \gg T_K) = 2\pi n_M S(S+1)j^2\rho(\epsilon_F)$, where $j = J/D$. When magnetic impurities are dilute, the Kondo effect screens the impurity spin for temperatures $T < T_K$. This results in a vanishing spin relaxation rate at zero temperature. At finite temperature the Kondo correlations enhance the spin relaxation rate, which becomes maximal at T_K . In weak-localization experiments a plateau in the temperature dependence of the dephasing time has been explained in terms of this peaked temperature dependent spin scattering from Kondo impurities^{190,191}, as numerically studied in Refs.^{98,192,193}. The following approximate expression is in good agreement with these results in all temperature regimes⁹⁷

$$\frac{1}{\tau_s^{(0)}}(T) = \frac{\pi n_m S(S+1)}{\rho} \left\{ \ln^2 \left(\frac{T}{T_K} \right) + \pi^2 S(S+1) \left[\left(\frac{T_K}{T} \right)^2 + \frac{1}{\beta} - 1 \right] \right\}^{-1} \quad (18)$$

Here, $\beta = 0.2^{193}$. Thus, the temperature dependence of $1/\tau_s(T)$ scales in the dilute limit with the Kondo temperature T_K . Note that, according to Eq. (18), the spin

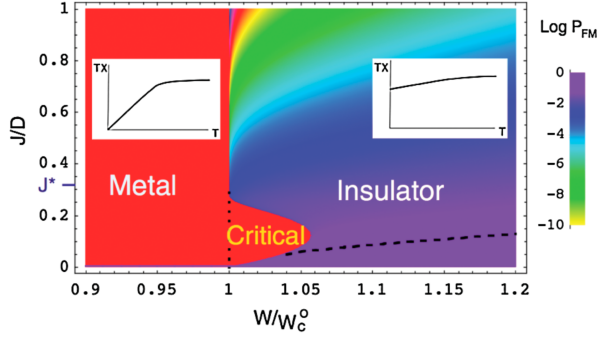


FIG. 7. Fraction of free MMs P_{FM} at $T = 0K$ in a 3D disordered metal as function of exchange coupling J (in units of band width D_0) and disorder strength W (in units of orthogonal critical value W_c^O). Critical correlations result in finite P_{FM} even for $J > J_c^A$, Eq. (22) (dashed line). For $J < J^*$ (as given by Eq. (21)) there is a critical region for disorder amplitudes $W_c^O < W < W_c^I(J)$, which is given by Eq. (20). Insets: schematic T -dependence of magnetic susceptibility χ times T . Fig. taken from Ref.¹⁹⁵, Copyright 2009, American Physical Society.

relaxation rate vanishes as T^2/T_K^2 in the low-temperature limit. Since this has the same temperature dependence as the inelastic scattering rate in a Fermi liquid this confirms the renormalized Fermi liquid theory of dilute Kondo systems, as formulated by Nozières¹⁹⁴.

At finite temperature T and in the presence of MMs the scaling Ansatz for the conductivity becomes therefore

$$\sigma(n, T) = \Delta n^{(d-2)\nu} F[T \Delta n^{-z\nu}, \tau_s^{-1}(T) \Delta n^{-\varphi_s}]. \quad (19)$$

Since MMs are Kondo screened in the metallic phase, while the Kondo screening can become quenched in the localised phase by the localisation length ξ_c , the spin scattering rate can be different in the metallic phase than in the insulator where free MMs remain. Therefore, in Refs.^{103,195} it was pointed out that there can emerge a new critical phase. The resulting quantum phase diagram was derived analytically, as shown in Fig. 7, where the concentration of free MMs at zero temperature is plotted. Furthermore, the temperature dependence of the spin relaxation rate results in finite temperature delocalization transitions^{103,195}. In Ref.¹⁰³ in the limit of dilute MMs the shift of the critical disorder as function of exchange coupling $j = J/D$ was found to be given by

$$W_c^I(j) = W_c^O + W_c^O \left(\frac{a_c^2}{D_e \tau_s^0} \right)^{\kappa(j)}, \quad (20)$$

where $1/\kappa(j) = \varphi_s - 2\nu \frac{d^2}{2\eta} (j + \eta/d)^2$. Here, the deviation of scaling from φ_s arises from the fact that the density of free MMs depends on localisation length $\xi \sim (W - W_c)^{-\nu}$, itself. This result is valid for dilute magnetic impurities, dominated by the Kondo effect and for small deviations from the orthogonal class value W_c^O . For larger exchange

couplings $j > j^*$, where

$$j^* = (2\sqrt{\eta} - \eta)/d, \quad (21)$$

(which is in $d = 3$, $j^* \approx 0.276$), the Kondo screening is no longer quenched, and the critical disorder W_c^I approaches the one of the orthogonal symmetry class W_c^O .

For a clean metallic system of finite size with finite number of states N , the Kondo renormalization is cutoff by the mean level spacing $\Delta = D_0/N$. The critical exchange coupling J_c below which the Kondo screening is quenched and the MMs remain free, vanishes then logarithmically with the number of states in the band, N , as $J_c \sim D_0/\ln N$. In an Anderson insulator the eigenstates at the Fermi energy are localized with a localization length ξ . Thus, there are finite local gaps of order $\Delta_{\xi_c} = (\rho \xi^d)^{-1}$ at the Fermi energy which cut off the Kondo renormalization and there are free MMs whenever $J < J_c^A$, where

$$J_c^A = D_0/\ln N_{\xi_c}, \quad (22)$$

with $N_{\xi_c} = D_0/\Delta_{\xi_c}$ the number of localized states with a finite wave function amplitude at the site of the MM¹¹². However, Eq. (22) does not take into account multifractality and critical correlations between wave functions at different energies at the AMIT¹⁰¹. In fact, the amplitude of multifractal states can be suppressed at some random positions below their typical value, scaling as $L^{-\alpha_\psi}$ with $\alpha_\psi > d$ (i.e., decaying faster with system size L than extended states). Correlations between wave functions at different energies then open wide local pseudogaps^{103,112}. The wave function intensities within a localization volume is close to log-normal distribution with $\alpha_\psi \rightarrow \alpha_{\psi, \xi} = -\ln |\psi|^2 / \ln \xi^{103}$. For the evaluation of J_c the system length L needs then to be substituted by the localization length $\xi(W) \sim (W - W_c)^{-\nu}$. Thus, for fixed J , the density of free MMs are found to depend on the localisation length ξ as¹⁰³

$$P_{\text{FM}} = n_{\text{FM}}/n_M = \text{Erfc} \left(\sqrt{\frac{\ln \xi}{2\eta/d}} \frac{J}{D} \right). \quad (23)$$

Close to the transition, where ξ is large, the density of free MMs Eq. (23) relative to n_M simplifies to $P_{\text{FM}} \sim (W - W_c)^{\kappa(J)}$ with positive exponent $\kappa(J) = (\nu/2\eta)(J/D)^2$. P_{FM} is plotted in Fig. 7 as function of disorder strength W and exchange coupling J . It is vanishing both in the metal and critical regions due to Kondo screening. In the insulator region it remains finite due to the quenching of the Kondo effect by localization and local pseudogaps. The critical region appears because for $j < j^*$ the position of the critical point W_c depends on the direction from which the AMIT is approached. Thus there exists a *critical phase* for intermediate disorder strengths $W_c^O < W < W_c^I(j)$. The width of that critical phase is $W_c^I(J) - W_c^O \sim n_M^{\kappa(j)}$, increasing with a power of the density of MMs, n_M ¹⁰³.

Magnetic field. One way to probe that quantum phase diagram is, to apply a magnetic field which polarizes the free MMs reducing thereby the spin relaxation rate^{192,196,197}. Also, the Kondo singlet is partially broken up by the Zeeman field. Thus, MMs contribute a spin relaxation rate which increases with the Zeeman field. An orbital magnetic field breaks time reversal symmetry and therefore results also in a shift of the AMIT, approaching the unitary limit. We found in Ref.¹⁰³ that the *Zeeman field* shifts the critical disorder to

$$W_c(B) = W_c^I(j) + W_c^O c_M \left(\frac{\gamma_s B |S_z|}{E_c} \right)^{j\kappa(j)}, \quad (24)$$

where $c_M = (dj n_M / ((2-j)\pi\rho D_e))^{\kappa(j)}$. Thus, one finds that the transition between the critical phase and the insulator is shifted in a magnetic field according to Eq. (24). The *orbital magnetic field* is known¹⁷⁶ to shift W_c to

$$W_c(B) = W_c^O + W_c^O (\pi e B / h)^{1/(2\nu)}. \quad (25)$$

This determines the transition line between metal and critical phase, since the Zeeman field contributes a slower dependence on B , coming from the metal side of the transition. For the transition between critical phase and insulator, we find that for $j < j_Z = \eta/d (2\sqrt{d+1+d^2/\eta/d} - 1 - 2/d)$, the shift of W_c is dominated by the Zeeman field. For, $d = 3, \eta/d = 2/3$ one finds, $j_Z = 0.185$. Thus the Zeeman field is dominating the shift of the transition for realistic values of exchange couplings j .

VII. FINITE TEMPERATURE DELOCALIZATION TRANSITIONS

Since the spin relaxation rate depends on temperature, Eq. (18), the breaking of the spin- and time-reversal-symmetry is found to depend on temperature, as well. Since we have seen above that the position of the AMIT is determined by the spin relaxation rate, it shifts as function of temperature T . Therefore, the metal-insulator transition can occur at a finite temperature $T_c(W, J)$. In order to investigate the existence of such a transition, we apply the Larkin-Khmelnitskii condition as outlined above^{176,178} with the temperature dependent symmetry parameter $X_s(T) = \xi^2 / D_e \tau_s(T)$ ¹⁰³.

Approaching the AMIT from the Insulator side. Coming from the insulating side of the transition, where the localization length ξ is still finite and smaller than the thermal length L_T , the ratio $X_s(T)$ is finite. $1/\tau_s(T)$ saturates at low temperatures to the spin relaxation rate from free MMs. Thus, at low temperatures the transition occurs at $W_c^I(J)$, as given by Eq. (20). Since the Kondo temperature is distributed, the spin relaxation rate at finite temperature is given by a weighted integral over its distribution function $P(T_K)$ as $1/\tau_s(T) =$

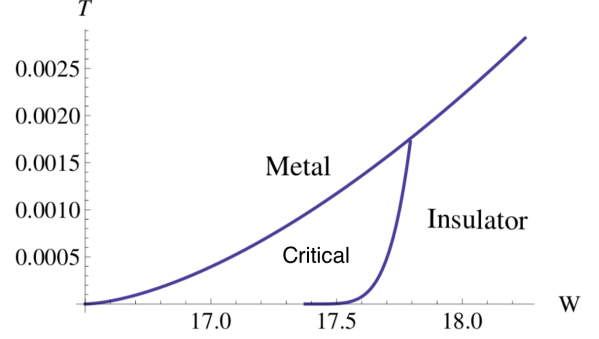


FIG. 8. (Color online) Finite-temperature phase diagram of Kondo-Anderson transitions. Plots of the critical temperatures $T_c^M(W, J)$, Eq. (27) (upper solid line), and $T_c^I(W, J)$, Eq. (26) (lower solid line), respectively, with disorder amplitude W in units of hopping parameter t and temperature in units of E_c , using $j = 0.2$, $\alpha_0 = 4$, $d = 3$, $\eta/d = 2/3$, $\nu = 1.57$ and $a_c^2 / (D_e \tau_s^{(0)}) = 0.1$. Fig. taken from Ref.¹⁰³, Copyright 2012, American Physical Society.

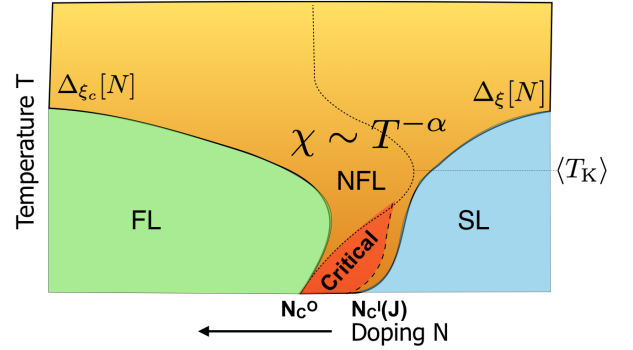


FIG. 9. Schematic phase diagram, with the crossover from Fermi liquid (FL) to non-FL behavior and a critical phase. The dashed lines are sketches of the critical concentration $N_c(T)$ which depends on temperature due to the temperature dependent spin scattering rate. It has a maximum at the average Kondo temperature $\langle T_K \rangle$, which is indicated by the dotted line. The critical phase forms since the spin scattering is different when coming from the metal, where MMs are Kondo screened and from the insulator side of the transition, where there are free MMs.

$\int_0^\infty dT_K P(T_K) 1/\tau_s(T/T_K)$. The spin relaxation rate of a magnetic impurity with a given Kondo temperature T_K , $1/\tau_s(T/T_K)$, is given by Eq. (18). Thus, it increases first like T^2/T_K^2 when $T < T_K$, reaching a maximum at T_K before it decays logarithmically towards its saturation value $1/\tau_s^0$. For low temperatures $T \ll T_K^0$, one can approximate $1/\tau_s(T)$ by a sum of the spin relaxation rate from free MMs at sites whose density of states is suppressed as $\rho(\mathbf{r}) \sim \xi^{d-\alpha_{FM}}$, and the spin relaxation from spins whose Kondo temperature exceeds T . From the scaling with $X_s(T)$ we can derive, as outlined above, the critical temperature $W_c^I(J, T)$, which thereby depends on

temperature T . As a consequence, we find a finite transition temperature between the insulator and an extended phase as

$$T_c^I = E_c c_I \left(\frac{W - W_c^I}{W_c^O} \right)^{\frac{1}{j}}, \quad (26)$$

where W_c^I is given by Eq. (20), and $c_I = (\kappa_j/j)^{-1/j} (D_e \tau_s^0)^{\kappa_j/j}$, where $1/\kappa_j = \nu(2 - d^2/2/\eta(j + \eta/d)^2)$. Eq. (26) is plotted in Fig. 8 (lower solid line).

Approaching the AMIT from the Metallic side. Coming from the metallic side, the density of free MMs decays at low temperatures $T < \Delta_\xi$ to zero. There, the spin relaxation rate is dominated by partially screened MMs with $T < T_K$. Thus, the transition is shifted to a different value, $W_c^M(T)$. Accordingly we find the transition temperature to the metal as

$$T_c^M(W) = \sqrt{S(S+1)\pi^2 D_e \tau_s^0} \left| \frac{W - W_c^O}{W_c^O} \right|^\nu T_K^0, \quad (27)$$

as is plotted in Fig. 8 (upper solid line) as function of disorder amplitude W .

Thus, we can conclude that in the dilute MM limit the temperature dependence of the spin scattering rate results in finite temperature transitions with critical temperatures $T_c^M(W)$, Eq. (27) and $T_c^I(W)$, Eq. (26). Since $T_c^M(W) \neq T_c^I(W)$ there is a critical region, as seen in Fig. 8. The corresponding finite temperature phase diagram as function of doping concentration N is shown in Fig. 9, schematically.

We note that this phase diagram is further complicated by the fact that $1/\tau_s$ reaches a maximum and decays to its saturation value logarithmically at temperatures exceeding the average Kondo temperature $\langle T_K \rangle$, as indicated schematically by the dotted line in Fig. 9. Furthermore, at higher temperature the phase boundaries are less well defined because of inelastic scattering and dephasing processes.

Finite Temperature Phase Diagram with Coupled MMs. The phase diagram shown in Fig. 9 is expected to be modified when the indirect exchange couplings between MMs dominate the Kondo effect for a finite concentration of MMs. Implementing both the Kondo screening and the effect of the RKKY couplings on the temperature dependence of the spin relaxation rate $1/\tau_s(T)$, as well as the doping dependence of the concentration of MMs, $n_M(N)$, as reviewed above, the finite temperature phase diagram of doped semiconductors can be derived. Furthermore, as reviewed above, there are strong indications that for any finite number of ferromagnetic couplings, as they are present close to the MIT, the coupled quantum spin system is driven to a fixed point with clusters forming large effective spins, contributing a Curie law magnetic susceptibility^{118,119}. Thus, there might be a finite concentration of such large effective spin clusters on both sides of the transition, which make the spin scattering rate $1/\tau_s$ finite. Then, the critical tongue found

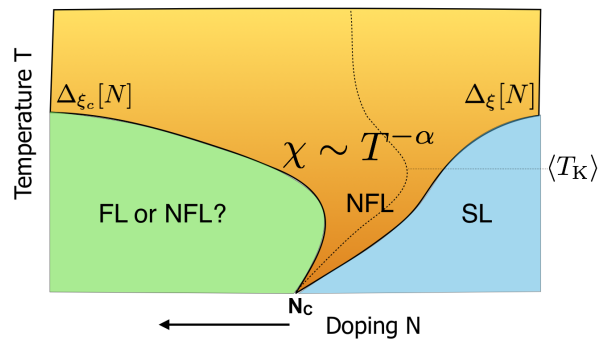


FIG. 10. Schematic phase diagram, in the presence of a finite concentration of MMs as function of doping concentration N and temperature T . The dashed line indicates the temperature dependence of the critical doping concentration $N_c(T)$ due to the temperature dependence of the spin scattering rate, $1/\tau_s(T)$ (It has a maximum at the average Kondo temperature $\langle T_K \rangle$, which is indicated by the dotted line.) This results in finite temperature transitions between the localised and the non-Fermi-liquid metallic phase. In the metallic phase, the competition between Kondo screening of local moments and indirect exchange coupling may in the low temperature limit $T < \Delta_{\xi_c}$ either lead to a disordered Fermi liquid or non-Fermi liquid, as indicated by the green area, in addition to the Althshuler-Aronov type corrections due to long range interactions⁷⁵⁻⁷⁷.

in the dilute MM limit as shown in Fig. 9, will be diminished at finite density of MMs. Still, as there will be a coexistence with a finite density of Kondo singlets and of random singlets, as reviewed above, the spin scattering rate $1/\tau_s(T)$ is expected to increase with temperature since the Kondo screened MMs and the random singlets, which do not contribute to spin scattering at low temperature, are increasingly broken up with increasing temperature T . Fig. 10 shows a sketch of the resulting expected phase diagram as function of doping concentration N and temperature T . Furthermore, the presence of clusters forming large effective spins, which contribute a Curie law magnetic susceptibility^{118,119}, and possibly also the presence of free MMs due to rare sites of dopant sites, which remain strongly isolated on the metallic side of the transition¹⁹, may result in a divergence of the magnetic susceptibility in the low temperature limit and non-Fermi liquid behavior, even at low temperatures $T < \Delta_{\xi_c}$, as indicated by a question mark in Fig. 10, in addition to the Althshuler-Aronov type corrections due to long range interactions⁷⁵⁻⁷⁷. This depends on the type of doping, and whether dopant locations are uncorrelated, as assumed in Ref.¹⁹ or so much correlated, that well isolated sites do not occur on the metallic side of the MIT.

VIII. CONCLUSIONS AND OUTLOOK

While still more experimental and theoretical research on doped semiconductors in the vicinity of the MIT is needed, we can conclude that it is now very well established that a finite density of magnetic moments are present in the vicinity of the MIT which need to be taken into account in a comprehensive theory of their MIT. These randomly positioned MMs can couple to form a spin liquid phase. This spin liquid phase is well established to occur in the insulating phase at low doping below the MIT, and at low temperatures, as shown schematically in blue in the phase diagram Fig. 10. This spin liquid is described very well by the Bhatt and Lee theory, where clusters of randomly coupled spins form, which, due to the random antiferromagnetic interactions at low doping, are mostly random singlets^{15,16}. The excitations of these random clusters of spins at finite temperature result in the anomalous power law divergence of the magnetic susceptibility $\chi(T) \sim T^{-\alpha}$, with $\alpha \leq 1$ ^{15,16}.

There is furthermore evidence for another region, the fan colored in orange in the phase diagram Fig. 10, where the doped semiconductor have also non-Fermi-liquid properties, as characterised, also by a divergent magnetic susceptibility, but which may be dominated by the formation of randomly distributed Kondo singlets. The agreement of the anomalous power α with the universal value Eq. (8), $\alpha = 1 - (\alpha_0 - 3)/3$, independent on the doping concentration N within this fan region, with the experimental results, as shown in the inset (circles) of Fig. 1⁸⁴ and results reported in Ref.⁶⁷, is striking. This universal value has been derived by taking into account multifractal correlations in the calculation of the local Kondo temperatures, which yields a distribution of Kondo temperatures with a power law tail Eq. (8) both at the MIT and in its vicinity on both sides of the transition. The fact that the resulting anomalous power of the magnetic susceptibility is experimentally found to be independent of doping close to the MIT and in good agreement with Eq. (8), as derived from multifractality, might make these experiments the first, albeit indirect, measurements of multifractality at the MIT in doped semiconductors.

Furthermore, temperature dependent spin correlations are found to cause finite temperature transitions between a localised and non-Fermi-liquid metallic phase. The critical doping concentration is found to depend on temperature, $N_c(T)$, due to the temperature dependence of the spin scattering rate $1/\tau_s(T)$, as indicated in Fig. 10, dotted line, which is caused by temperature dependent spin correlations, such as the Kondo effect. The question arises how to detect these finite temperature MITs experimentally. Neglecting the coupling to phonons, one would have a transition between zero conductivity $\sigma(T) = 0$ at $T < T_c(N, J)$ and a metal with finite conductivity $\sigma(T) > 0$ at $T > T_c(N, J)$. Thus, that makes it similar

to the finite temperature many body localization (MBL) transitions, which were suggested in Refs¹⁹⁸ and¹⁹⁹ and implied in the work Ref.²⁰⁰, where arguments were presented that short-range interactions in an electron system with localized single-particle states might not destroy localization for some range of finite temperature T . MBL is meanwhile also understood to manifest itself by the lack of thermalization, see Refs.^{201,202}. With phonon scattering one expects for $T < T_c(N, J)$ an exponentially low conductivity, as described by the Efros-Shklovskii variable range hopping conductivity⁷⁹. The application of a magnetic field is expected to strongly change the phase diagram and thereby lead to giant magneto conductivity, since the critical disorder, Eq. (24), and respectively, the critical dopant density of the transition depends on the magnetic field. Further theoretical research and experiments on doped semiconductors will be needed to explore and understand the finite temperature diagram as function of doping and magnetic field completely and resolve remaining open problems which include: It is not yet clear whether and under which conditions the random Kondo singlet phase can become quenched by indirect exchange interactions between magnetic moments. While there is strong evidence that the supercritical low temperature phase is dominated by long range Coulomb interactions which are only partially screened due to disorder⁷⁸, it remains to be understood under which conditions a spin liquid phase of magnetic moments may persist in this disordered metal phase¹⁹.

ACKNOWLEDGMENTS

This review reflects my personal perspective achieved through fruitful collaborations and discussions with Ravin Bhatt, Georges Bouzerar, Konstantin B. Efetov, Peter Fulde, Jean-Francois Guillemales, Stephan Haas, Ki-Seok Kim, Bernhard Kramer, Alexander Lichtenstein, Hu-Jong Lee, Hyun-Yong Lee, Youcef Mohdeb, Eduardo R. Mucciolo, Tomi Ohtsuki, Mikhail Raikh, Vincent Sacksteder, Keith Slevin, Alexey Tselvick, Javad Vahedi, Imre Varga and Isa Zharekeshev, which I gratefully acknowledge, and thanks to insightful discussions with Elihu Abrahams, Kamran Behnia, Claudio Chamon, Vladimir Dobrosavljevic, Alexander M. Finkel'shtein, Serge Florens, Hans Kroha, Raj Mohanty, Cécile Monthus, Philippe Nozières and Christoph Strunk. I am grateful to Ki-Seok Kim and Tomi Ohtsuki for critical reading of the manuscript and useful comments. I am particularly grateful to Konstantin B. Efetov for introducing me to the fascinating field of disordered systems while being his PhD student and then his Post Doc, and for his guidance and comprehensive advice²⁰³ ever since. Support from DFG (Deutsche Forschungsgemeinschaft) KE-807/22-1 is gratefully acknowledged.

- ¹ T. F. Rosenbaum, R. F. Milligan, M. A. Paalanen, G. A. Thomas, R. N. Bhatt, and W. Lin Phys. Rev. B **27**, 7509 (1983).
- ² R. F. Milligan, T. F. Rosenbaum, R. N. Bhatt, G.A.Thomas, Modern Problems in Condensed Matter Sciences, **10**, 231 (1985).
- ³ H. von Löhneysen, Ann. Phys. (Berlin) **523**, 599 (2011).
- ⁴ R.N. Bhatt and S. Kettemann Ann. of Phys. **435** , 168664 (2021).
- ⁵ P. W. Anderson, Phys. Rev. **109**, 1492 (1958); Nobel Lectures in Phys. **1980**, 376 (1977).
- ⁶ N. Mott, Rev. Mod. Phys. **40**, 677 (1968); N. F. Mott, J. Phys. Colloques **37**, 301 (1976)
- ⁷ P. A. Lee, and T. V. Ramakrishnan, Rev. Mod. Phys. **57**, 287 (1985).
- ⁸ B. Kramer, and A. MacKinnon, Reports on Prog. Phys. **56**, 1469 (1993).
- ⁹ D. Belitz, and T. Kirkpatrick, Rev. Mod. Phys. **66** (1994).
- ¹⁰ K. B. Efetov, Adv. Phys. **32**, 53 (1983)
- ¹¹ K. B. Efetov, Supersymmetry in Disorder and Chaos, Cambridge University Press, Cambridge, 1997.
- ¹² F. Evers, and A. Mirlin, Rev. Mod. Phys. **80**, 63 (2008).
- ¹³ F. Wegner, Z. Phys. **B 25**, 327 (1976).
- ¹⁴ K. Andres, R. N. Bhatt, P. Goalwin, T. M. Rice, and R. E. Walstedt, Phys. Rev. B **24**, 244 (1981).)
- ¹⁵ R. N. Bhatt and P. A. Lee, Journal of Applied Physics **52**, 1703-1707 (1981).
- ¹⁶ R. N. Bhatt and P. A. Lee, Phys. Rev. Lett. **48**, 344(1982).
- ¹⁷ M. A. Paalanen, J. E. Graebner, R. N. Bhatt, and S. Sachdev, Phys. Rev. Lett. **61**, 597 (1988).
- ¹⁸ S. Sachdev, Phys. Rev. B **39**, 5297 (1989).
- ¹⁹ R. N. Bhatt and D. S. Fisher, Phys. Rev. Lett. **68**, 3072 (1992).
- ²⁰ M. Lakner, H. v. Löhneysen, A. Langenfeld and P. Wölfle, Phys. Rev. B **50**, 17064 (1994).
- ²¹ E. Miranda and V. Dobrosavljevic, Reports on Progress in Physics **68**, 2337 (2005).
- ²² X. Lin, Z. Zhu, B. Fauqué, and K. Behnia, Phys. Rev. **X 3**, 021002 (2013).
- ²³ M.R. Norman, C. Pépin, Rep. Progr. Phys. **66** (10),1547 (2003).
- ²⁴ D. van der Marel, H. J. A. Molegraaf, J. Zaanen, Z. Nussinov, F. Carbone, A. Damascelli, H. Eisaki, M. Greven, P. H. Kes, and M. Li, Nature (London) **425**, 271 (2003).
- ²⁵ P.A. Lee, N. Nagaosa, X.-G. Wen, Rev. Modern Phys. **78**, 17 (2006) .
- ²⁶ E. Fradkin, S.A. Kivelson, J.M. Tranquada, Rev. Modern Phys. **87**, 457 (2015).
- ²⁷ C. Pépin a, H. Freire, Ann. of Phys., **169233**, (2023).
- ²⁸ M. Z. Hasan and C. L. Kane, Rev. Mod. Phys. **82**, 3045 (2010).
- ²⁹ M. S. Foster and E. A. Yuzbashyan, Phys. Rev. Lett. **109**, 246801 (2012).
- ³⁰ T. I. Baturina, A. Yu. Mironov, V. M. Vinokur, M. R. Baklanov, and C. Strunk Phys. Rev. Lett. **99**, 257003 (2007).
- ³¹ K. Sato, L. Bergqvist, J. Kudrnovský, P. H Dederichs, O. Eriksson, I. Turek, B. Sanyal, G. Bouzerar, H. Katayama-Yoshida, V. A. Dinh, T. Fukushima, H. Kizaki, R. Zeller, Reviews of Modern Physics **82** (2), 1633 (2010).
- ³² S. Kettemann and J. F. Guillemoles, in Proceedings of the 13th European Photovoltaic Solar Energy Conference, Nice, 119 (1995).
- ³³ A. Luque and A. Marti, Phys. Rev. Lett. **78**, 5014 (1997).
- ³⁴ Y. Okada, N. J. Ekins-Daukes, T. Kita, R. Tamaki, M. Yoshida, A. Pusch, O. Hess, C. C. Phillips, D. J. Farrell, K. Yoshida, N. Ahsan, Y. Shoji, T. Sogabe, and J.-F. Guillemoles, Applied Physics Reviews **2**, 021302 (2015).
- ³⁵ J. Nelson, Phys. Rev. B **59**, 15374 (1999).
- ³⁶ M. T. Agne, F. R. L. Lange, J. P. Male, K. S. Siegert, H. Volker, C. Poltorak, A. Poitz, T. Siegrist, S. Maier, G. J. Snyder, M. Wuttig, Matter, **4**, 2970-2984, (2021).
- ³⁷ C. Castellani, C. Di Castro, M. Grilli and G. Strinati, Phys. Rev. B **37**, 6663 (1988).
- ³⁸ C. Villagonzalo, R. Römer and M. Schreiber, Eur. Phys. J. **B 12**, 179 (1999).
- ³⁹ H. Stupp, M. Hornung, M. Lakner, O. Madel, H. von Löhneysen, Phys. Rev. Lett. **72**, 2122 (1994).
- ⁴⁰ S.Bogdanovich, M. P. Sarachik, R. N. Bhatt, Phys. Rev. Lett. **82**,137 (1999).
- ⁴¹ K. M. Itoh, M. Watanabe, Y. Ootuka, E. E. Haller, and T. Ohtsuki, J. of Phys. Soc. Japan **73**, 173 (2004).
- ⁴² N. F. Mott, The Philosophical Magazine: A, Journal of Theoretical Experimental and Applied Physics, **6:62**, 287-309 (1961).
- ⁴³ A. Möbius, J. Phys. C **18**, 4638 (1985); Phys. Rev. B **40**, 4194 (1989).
- ⁴⁴ M. A. Paalanen, G. A. Thomas, Helv. Phys. Acta **56**, 27 (1983).
- ⁴⁵ E. Abrahams, P. W. Anderson, D. C. Licciardello, and T. V. Ramakrishnan, Phys. Rev. Lett. **42**, 673 (1979).
- ⁴⁶ D. Thouless, Phys. Rep., Phys. Lett. **13**, 93 (1974).
- ⁴⁷ F. Wegner, Z. Phys. B **35**, 207 (1979).
- ⁴⁸ K. B. Efetov, A. I. Larkin and D. E. Khmeniskii, Sov. Phys. JETP **52**, 568 (1980).
- ⁴⁹ K. Jüngling, and R. Oppermann, Z. Phys. **B 38**, 93 (1980).
- ⁵⁰ L. Schaefer and F. Wegner, Z. Phys. **B 38**, 113 (1980).
- ⁵¹ L. P. Gorkov, A. I. Larkin and D. Khmel'nitskii, JETP Lett. **30**, 248 (1979).
- ⁵² D. Vollhardt, and P. Wölfle, Phys. Rev. **B 22**, 4666 (1980).
- ⁵³ S. Hikami, Nucl. Phys. **B 215** FS7 555 (1983).
- ⁵⁴ F. Wegner, Nucl. Phys. **B 316**, 663 (1989).
- ⁵⁵ S. Hikami, Progress of Theoretical Physics Supplement **107**, 213 (1992).
- ⁵⁶ K. B. Efetov, Sov. Phys. JETP **61**, 606 (1985).
- ⁵⁷ K. B. Efetov, Sov. Phys. JETP **65**, 360 (1987).
- ⁵⁸ M. R. Zirnbauer, Phys. Rev. B **34**, 6394 (1986); M. R. Zirnbauer, Nucl. Phys. B **265**, 375 (1986).
- ⁵⁹ A. D. Mirlin and Y. V. Fyodorov, Nucl. Phys. B **366**, 507 (1991).
- ⁶⁰ K. B. Efetov, Physica **A 167**, 119-131 (1990).
- ⁶¹ Y. V. Fyodorov, A. D. Mirlin and H.-J. Sommers, J. Phys. I **2**, 1571 (1992).
- ⁶² S. Hikami, arXiv:1811.05918 (2018).
- ⁶³ K. Slevin, and T. Ohtsuki, New J. Phys. **16**, 015012 (2014).
- ⁶⁴ A. Rodriguez, L. J. Vasquez, K. Slevin, and R. A. Römer, Phys. Rev. B **84**, 134209 (2011).
- ⁶⁵ P. W. Anderson, Phys. Rev. **124**, 41(1961).

- ⁶⁶ Y. Toyozawa, J. Phys. Soc. Jpn. **17**, 986-1004 (1962).
- ⁶⁷ R. Bhatt, M. Paalanen, S. Sachdev, J. de Phys. Coll. **49** C8-1179 (1988).
- ⁶⁸ D. Jung, K. Slevin, S. Kettemann, Phys. Rev. B **93**, 134203 (2016).
- ⁶⁹ Y. Harashima, K. Slevin, Phys. Rev. B **89**, 205108 (2014).
- ⁷⁰ M. Amini, V. E. Kravtsov, M. Mueller, New J. Phys. **16**, 015022 (2014).
- ⁷¹ H. Terletska, Y. Zhang, K.-M. Tam, T. Berlijn, L. Chioncel, N. S. Vidhyadhiraja, and M. Jarrell, Appl. Sci. **8**, 2401 (2018).
- ⁷² E. G. Carnio, N. D. M. Hine, and R. A. Römer, Physical Review B, **99**, 081201(R) (2019).
- ⁷³ J. Chabé, G. Lemarié, B. Grémaud, D. Delande, P. Szriftgiser and J. G. Garreau, Phys. Rev. Lett. **101**, 255702 (2008).
- ⁷⁴ M. Lopez, J.-F. Clément, P. Szriftgiser, J. C. Garreau and D. Delande, Phys. Rev. Lett. **108**, 095701 (2012).
- ⁷⁵ B. Altshuler, A. Aronov, JETP **50**, 968 (1980).
- ⁷⁶ A. M. Finkel'shtein, Sov. Phys. JETP, 57(1), 97-108 (1983); JETP Lett. **37**, 517 (1983); *ibid.* **40**, 796 (1984).
- ⁷⁷ A. M. Finkel'shtein, J. Phys. Coll. **49**, C8-1173 (1988).
- ⁷⁸ A. M. Finkel'shtein, G. Schwiete, Ann. of Phys., 169260 (2023).
- ⁷⁹ A. L. Efros and B. I. Shklovskii, J. Phys. **C 8**, L49 (1975).
- ⁸⁰ J. D. Quirt and J. R. Marko, Phys. Rev. B **7**, 3842 (1973); R. Marito, P. Harrison, and D. Quirt, Phys. Rev. B **10**, 2448 (1974).
- ⁸¹ N. Kobayashi, S. Ikehata, S. Kobayashi, and W. Sasaki, Solid State Commun. **24**, 67 (1977); **32**, 1147 (1979).
- ⁸² H. Alloul and P. Dellouve, Phys. Rev. Lett. **59**, 578 (1987)
- ⁸³ A. Roy and M.P. Sarachik, Phys. Rev. **8** 37, 5531 (1988)
- ⁸⁴ H. Schlager, and H. Löhneysen, Europhys. Lett. **661** (1997).
- ⁸⁵ M.J. Hirsch, D.F. Holcomb, R.N. Bhatt, and M.A. Paalanen, Phys. Rev. Lett., 1418 (1992).
- ⁸⁶ M. Milovanović, S. Sachdev, and R. N. Bhatt, Phys. Rev. Lett. **63**, 82 (1989).
- ⁸⁷ A. M. Finkel'shtein, JETP Lett. **46**, 513 (1987).
- ⁸⁸ J. Kondo, Progr. Theor. Phys. **32**, 37 (1964).
- ⁸⁹ Y. Nagaoka, Phys. Rev. **A 138**, 1112 (1965).
- ⁹⁰ H. Suhl, Phys. Rev. **A 138**, 515 (1965).
- ⁹¹ K.G. Wilson, Rev. Mod. Phys. **47**, 773 (1975).
- ⁹² A. M. Tsvelick and P. B. Wiegmann, Adv. Phys. **32**, 453 (1983); N. Andrei, K. Furuya, and J. H. Lowenstein, Rev. Mod. Phys. **55**, 331 (1983).
- ⁹³ K. Maki, Progr. Theor. Phys. **41**, 586 (1969); J. Kopp, J. Phys. **F 5**, 1211 (1975).
- ⁹⁴ M. Lakner and H. v. Löhneysen, Phys. Rev. Lett. **70**, 3475 (1993).
- ⁹⁵ A. Langenfeld and P. Wölfle, Ann. Physik **4**, 43 (1995).
- ⁹⁶ V. Dobrosavljevic, T. R. Kirkpatrick, and G. Kotliar, Phys. Rev. Lett. **69**, 1113 (1992); E. Miranda, V. Dobrosavljevic, and G. Kotliar, *ibid.* **78**, 290 (1997).
- ⁹⁷ S. Kettemann and E. R. Mucciolo, JETP Lett. **83**, 240 (2006) [Pis'ma v ZhETF **83**,284 (2006)].
- ⁹⁸ T. Micklitz, A. Altland, T. A. Costi, and A. Rosch, Phys. Rev. Lett. **96**, 226601 (2006).
- ⁹⁹ S. Kettemann, E. R. Mucciolo, Phys. Rev. B **75**, 184407 (2007).
- ¹⁰⁰ F. Wegner, Z. Phys. B **36**, 209 (1980); H. Aoki, J. Phys. C **16**, L205 (1983); C. Castellani and L. Peliti, J. Phys. A **19**, L991 (1986); M. Schreiber and H. Grubbach, Phys. Rev. Lett. **67**, 607 (1991); M. Janssen, Int. J. Mod. Phys. B **8**, 943 (1994).
- ¹⁰¹ J. T. Chalker, Physica A (Amsterdam) **167**, 253 (1990); V. E. Kravtsov and K. A. Muttalib, Phys. Rev. Lett. **79**, 1913 (1997); J. T. Chalker *et al.*, JETP Lett. **64**, 386 (1996); T. Brandes, B. Huckestein, L. Schweitzer, Ann. Phys. (Leipzig) **5**, 633 (1996); V. E. Kravtsov, *ibid.* **8**, 621 (1999); V. E. Kravtsov, A. Ossipov, O. M. Yevtushenko, and E. Cuevas, Phys. Rev. B **82**, 161102 (2010); V. E. Kravtsov, A. Ossipov, O. M. Yevtushenko, J. Phys. A **44**, 305003 (2011).
- ¹⁰² E. Cuevas and V. E. Kravtsov, Phys. Rev. B **76**, 235119 (2007).
- ¹⁰³ S. Kettemann, E. R. Mucciolo, I. Varga, K. Slevin, Phys. Rev. B **85**, 115112 (2012).
- ¹⁰⁴ S. Kettemann, Phys. Rev. Lett. **117**, 146602 (2016).
- ¹⁰⁵ M. V. Feigel'man, L. B. Ioffe, V. E. Kravtsov, and E. A. Yuzbashyan, Phys. Rev. Lett. **98**, 027001 (2007); M. V. Feigel'man, L. B. Ioffe, V. E. Kravtsov, E. Cuevas, Annals of Physics **325**, 1368 (2010).
- ¹⁰⁶ E. G. Carnio, N. D. M. Hine, and R. A. Römer, Physica E: Low-Dimensional Systems and Nanostructures **111**, 141-147 (2019).
- ¹⁰⁷ I. S. Burmistrov, I.V. Gornyi, A.D. Mirlin, Phys. Rev. Lett. **111**, 066601 (2013).
- ¹⁰⁸ I. S. Burmistrov, I.V. Gornyi, A.D. Mirlin, JETP Lett. **106**, 272 (2017).
- ¹⁰⁹ A. Weisse, G. Wellein, A. Alvermann, H. Fehske, Rev. Mod. Phys. **78**, 275 (2006).
- ¹¹⁰ K. Slevin, S. Kettemann, T. Ohtsuki, Eur. Phys. J. **B 92**, 281(2019).
- ¹¹¹ P. S. Cornaglia, D. R. Grempel, and C. A. Balseiro, Phys. Rev. Lett. **96**, 117209 (2006).
- ¹¹² A. Zhuravlev, I. Zharekeshv, E. Gorelov, A. I. Lichtenstein, E. R. Mucciolo, and S. Kettemann, Phys. Rev. Lett. **99**, 247202 (2007).
- ¹¹³ M. Debertolis, I. Snyman, and S. Florens Phys. Rev. B **106**, 125115 (2022).
- ¹¹⁴ S. Kettemann and M. E. Raikh, Phys. Rev. Lett. **90**, 146601 (2003).
- ¹¹⁵ F. Igloi, C. Monthus, Phys. Rep. **412**, 277 (2005).
- ¹¹⁶ M. A. Ruderman and C. Kittel, Phys. Rev. **96**, 99 (1954); T. Kasuya, Prog. Theor. Phys. **16**, 45 (1956); K. Yosida, Phys. Rev. **106**, 893 (1957).
- ¹¹⁷ E. Westerberg, A. Furusaki, M. Sigrist, and P. A. Lee, Phys. Rev. B **55**, 12578 (1997); Phys. Rev. Lett. **75**, 4302 (1995).
- ¹¹⁸ B. Frischmuth, M. Sigrist, B. Ammon, M. Troyer, Phys. Rev. B **60**, 003388 (1999).
- ¹¹⁹ X. Wan, K. Yang, R. N. Bhatt, Phys. Rev. B, **66**, 014429 (2002).
- ¹²⁰ O. Motrunich, S.-C. Mau, and D. A. Huse, D. S. Fisher, Phys. Rev. B **61**, 1160 (2000).
- ¹²¹ I. V. Lerner, Phys. Rev. B **48**, 9462 (1993).
- ¹²² P. G. de Gennes, J. Phys. Radium **23**, 630 (1962).
- ¹²³ H. Y. Lee, S. Kettemann, Phys. Rev. B **89**, 165109 (2014).
- ¹²⁴ R. Juhász, I. A. Kovács, and F. Igloi, EPL (Europhysics Letters) **107**, 47008 (2014).
- ¹²⁵ N. Moure, S. Haas, and S. Kettemann, EPL (Europhysics Letters) **111**, 27003 (2015).
- ¹²⁶ N. Moure, H.-Y. Lee, S. Haas, R. N. Bhatt, and S. Kettemann, Phys. Rev. B **97**, 014206 (2018).
- ¹²⁷ Y. Mohdeb, J. Vahedi, N. Moure, A. Roshani, H.-Y. Lee, R. N. Bhatt, S. Kettemann, and S. Haas, Physical Review B **102**, 214201 (2020).

- ¹²⁸ R. Juhász, Phys. Rev. **B** **104**, 054209 (2021).
- ¹²⁹ Y. Mohdeb, J. Vahedi, S. Kettemann, Phys. Rev. **B** **106**, 104201 (2022).
- ¹³⁰ A. J. Bray and M. A. Moore, J. Phys. C **13**, L655 (1980).
- ¹³¹ S. Sachdev and J. Ye, Phys. Rev. Lett. **70**, 3339 (1993).
- ¹³² A. Y. Kitaev, Talks at KITP, University of California, Santa Barbara, entanglement in strongly-correlated quantum matter (2015), <https://online.kitp.ucsb.edu/online/entangled15/>.
- ¹³³ S. Sachdev, Phys. Rev. **X** **5**, 041025 (2015).
- ¹³⁴ Y. Gu, A. Kitaev, S. Sachdev, and G. Tarnopolsky, Notes on the complex Sachdev-Ye-Kitaev model, J. High Energy Phys. **02** (2020) 157.
- ¹³⁵ D. Chowdhury, A. Georges, O. Parcollet and S. Sachdev, Rev. Mod. Phys. **94**, 035004 (2022).
- ¹³⁶ D. Bagrets, A. Altland and A. Kamenev, Power-law out of time order correlation functions in the SYK model, Nucl. Phys. **B** **921**, 727 (2017).
- ¹³⁷ T. A. Sedrakyan and K. B. Efetov Phys. Rev. **B** **102**, 075146 (2020).
- ¹³⁸ C. M. Varma, P. B. Littlewood, S. Schmitt-Rink, E. Abrahams, and A. E. Ruckenstein Phys. Rev. Lett. **63**, 1996 (1989).
- ¹³⁹ M. Christos, F. M. Haehl and S. Sachdev, Phys. Rev. **B** **105**, 085120 (2022).
- ¹⁴⁰ D. Sherrington and S. Kirkpatrick, Phys. Rev. Lett. **35**, 1792 (1975).
- ¹⁴¹ R. Fisch, Phys. Rev. B **22**, 3459 (1980).
- ¹⁴² B. L. Dwyer, L. V. H. Rodgers, E. K. Urbach, D. Bluvstein, S. Sangtawesin, H. Zhou, Y. Nassab, M. Fitzpatrick, Z. Yuan, K. De Greve, E. L. Peterson, H. Knowles, T. Sumarac, J.-P. Chou, A. Gali, V.V. Dobrovitski, M. D. Lukin, and N. P. de Leon, PRX Quantum **3**, 040328 (2022).
- ¹⁴³ E. J. Davis, B. Ye, F. Machado, S. A. Meynell, W. Wu, T. Mittiga, W. Schenken, M. Joos, B. Kobrin, Y. Lyu, Z. Wang, D. Bluvstein, S. Choi, C. Zu, A. C. Bleszynski Jayich, N. Y. Yao, arXiv:2103.12742v3 quant-ph (2022).
- ¹⁴⁴ A. Signoles, T. Franz, R. F. Alves, M. Gärttner, S. Whitlock, G. Zürn, and M. Weidemüller, Phys. Rev. X **11**, 011011 (2021).
- ¹⁴⁵ A. Browaeys and T. Lahaye, Nature Physics **16**, 132 (2020).
- ¹⁴⁶ T. Franz, S. Geier, C. Hainaut, A. Signoles, N. Thaçharoen, A. Tebben, A. Salzinger, A. Braemer, M. Gärttner, G. Zürn, and M. Weidemüller, arXiv arXiv.2207.14216 (2022).
- ¹⁴⁷ R. Islam, C. Senko, W. C. Campbell, S. Korenblit, J. Smith, A. Lee, E. E. Edwards, C.C. J. Wang, J. K. Freericks, and C. Monroe, Science **340**, 583 (2013).
- ¹⁴⁸ P. Richerme, Z.-X. Gong, A. Lee, C. Senko, J. Smith, M. Foss-Feig, S. Michalakis, A. V. Gorshkov, and C. Monroe, Nature **511**, 198 (2014).
- ¹⁴⁹ P. Jurcevic, B. P. Lanyon, P. Hauke, C. Hempel, P. Zoller, R. Blatt, and C. F. Roos, Nature **511**, 202 (2014).
- ¹⁵⁰ S. Doniach, Physica **B+C** **91**, 231 (1977).
- ¹⁵¹ H. Kroha, *Modeling and Simulation* **7**, 12.1-12.27 (Verlag Forschungszentrum Julich), ISBN 978-3-95806-224-5 (2017).
- ¹⁵² S. G. Magalhaes, F. M. Zimmer, P. R. Krebs and B. Coqblin, Phys. Rev. B **74**, 014427 (2006); B. Coqblin, J. R. Iglesias, N. B. Perkins, S. G. Magalhaes and F. M. Zimmer, J. Magn. Magn. Mater. **320**, 1989 (2008).
- ¹⁵³ S. Burdin and P. Fulde, Phys. Rev. **B** **76**, 104425 (2007).
- ¹⁵⁴ B. Poudel, G. Zwirnagl, C. Lacroix, S. Burdin, J. of Magnetism and Magnetic Materials **520**, 167405 (2021)
- ¹⁵⁵ K. Byczuk, W. Hofstetter, U. Yu, and D. Vollhardt, Eur. Phys. J. Spec. Top **180**, 135 (2009).
- ¹⁵⁶ M. Ulmke, V. Janis, and D. Vollhardt, Phys. Rev. B **51**, 10411 (1995).
- ¹⁵⁷ M. C. O. Aguiar, V. Dobrosavljevic, E. Abrahams, and G. Kotliar, Phys. Rev. B **73**, 115117 (2006).
- ¹⁵⁸ M. C. O. Aguiar, V. Dobrosavljevic, E. Abrahams, and G. Kotliar, Phys. Rev. Lett. **102**, 156402 (2009).
- ¹⁵⁹ D. Tanaskovic, V. Dobrosavljevic, E. Abrahams, and G. Kotliar, Phys. Rev. Lett. **91**, 066603 (2003).
- ¹⁶⁰ M. C. O. Aguiar and V. Dobrosavljevic, Phys. Rev. Lett. **110**, 066401 (2013).
- ¹⁶¹ K. Byczuk, W. Hofstetter, and D. Vollhardt, Phys. Rev. Lett. **94**, 056404 (2005).
- ¹⁶² A. Weh, Y. Zhang, A. Östlin, H. Terletska, D. Bauernfeind, K.-M. Tam, H. G. Evertz, K. Byczuk, D. Vollhardt, and L. Chioncel, Phys. Rev. **B** **104**, 045127 (2021).
- ¹⁶³ S. Sachdev, Phil. Trans. R. Soc. A **356**, 173 (1998).
- ¹⁶⁴ M. A. Tusch and D. E. Logan, Phys. Rev. B **48**, 14843 (1993).
- ¹⁶⁵ P. B. Chakraborty, K. Byczuk, and D. Vollhardt, Phys. Rev. B **84**, 035121 (2011).
- ¹⁶⁶ M. Ulmke and R. T. Scalettar, Phys. Rev. B **55**, 4149 (1997).
- ¹⁶⁷ M. E. Pezzoli and F. Becca, Phys. Rev. **B** **81**, 075106 (2010).
- ¹⁶⁸ S. Sen, N. S. Vidhyadhiraja, M. Jarrell, Phys. Rev. B **98**, 075112 (2018).
- ¹⁶⁹ C. E. Ekuma, H. Terletska, K.-M. Tam, Z.-Y. Meng, J. Moreno, et al., Phys. Rev. B **89**, 081107 (2014).
- ¹⁷⁰ A. Nejati, K. Ballmann, J. Kroha, Phys. Rev. Lett. **118**, 117204 (2017).
- ¹⁷¹ K.-Y. Park, I. Jang, K.-S. Kim, S. Kettemann, Ann. of Phys. **435**, 168501 (2021).
- ¹⁷² G. Zarand and L. Udvardi, Phys. Rev. B **54**, 7606 (1996).
- ¹⁷³ D. Withoff and E. Fradkin, Phys. Rev. Lett. **64**, 1835 (1990); K. Ingersent, Phys. Rev. B **54**, 11936(1996).
- ¹⁷⁴ W. Zhang, E. R. Brown, and R. P. Mirin, Phys. Rev. Research **4**, 043040 (2022).
- ¹⁷⁵ S. Hikami, A. Larkin, and Y. Nagaoka, Prog. Theor. Phys. **63**, 707 (1980).
- ¹⁷⁶ D. Khmel'nitskii, and A. Larkin, Solid State Commun. **39**, 1069 (1981).
- ¹⁷⁷ F. J. Wegner, Nucl. Phys. B **270**, 1 (1986).
- ¹⁷⁸ T. Dröse, M. Batsch, I. K. Zharekeshv, and B. Kramer, Phys. Rev. B **57**, 37 (1998).
- ¹⁷⁹ A.V. Kolesnikov and K.B. Efetov, Phys. Rev. Lett. **83**, 3689 (1999).
- ¹⁸⁰ A.V. Kolesnikov and K.B. Efetov, <https://arxiv.org/abs/cond-mat/0005101v3> (2020).
- ¹⁸¹ J.L. Pichard, M. Sanquer, K. Slevin, and P. Debray, Phys. Rev. Lett. **65**, 1812, (1990).
- ¹⁸² H. Schomerus and C.W.J. Beenakker, Phys. Rev. Lett. **84**, 3927 (2000).
- ¹⁸³ M. Weiss, T. Kottos and T. Geisel, Phys. Rev. B **63**, 081306(R) (2001).
- ¹⁸⁴ J. P. Bouchaud, J. Phys. **I** **1**, 985(1991).
- ¹⁸⁵ I.V. Lerner and Y. Imry, Europhys. Lett. **29**, 49 (1995).
- ¹⁸⁶ S. Kettemann, Phys. Rev. **B** Rapid Communications **62**, R13282 (2000).

- ¹⁸⁷ M. E. Gershenson, Yu. B. Khavin, A. G. Mikhalchuk, H.M. Bozler, and A. L. Bogdanov, Phys. Rev. Lett. **79**, 725 (1997); Yu. B. Khavin, M. E. Gershenson, and A. L. Bogdanov, Phys. Rev. **B 58**, 8009 (1998).
- ¹⁸⁸ S. Kettemann, Phys. Rev. **B 69**, 035339 (2004).
- ¹⁸⁹ S. Hikami, Prog. Theor. Phys. **64**, 1466 (1980).
- ¹⁹⁰ G. Bergmann, Phys. Rev. Lett. **58**, 1236 (1987); R. P. Peters, G. Bergmann, and R. M. Mueller, *ibid.* **58**, 1964 (1987); C. Van Haesendonck, J. Vranken, and Y. Bruynseraede, *ibid.* **58**, 1968 (1987).
- ¹⁹¹ P. Mohanty and R. A. Webb, Phys. Rev. Lett. **84**, 4481 (2000).
- ¹⁹² T. Micklitz, T. A. Costi, and A. Rosch, Phys. Rev. **B 75**, 054406 (2007).
- ¹⁹³ G. Zaránd, L. Borda, J. von Delft, and N. Andrei, Phys. Rev. Lett. **93**, 107204 (2004).
- ¹⁹⁴ P. Nozières, J. Low Temp. Phys. **17**, 3 (1974).
- ¹⁹⁵ S. Kettemann, E. R. Mucciolo, and I. Varga, Phys. Rev. Lett. **103**, 126401 (2009).
- ¹⁹⁶ A.A. Bobkov, V.I. Falko, and D.E. Khmel'nitskii, Zh. Exp. Teor. Fiz. **98**, 703 (1990) [Sov. Phys. JETP **71**, 393 (1990)].
- ¹⁹⁷ M.G. Vavilov, L.I. Glazman, Phys. Rev. **B 67**, 115310 (2003); M. G. Vavilov, L. I. Glazman, and A. I. Larkin, Phys. Rev. **B 68**, 075119 (2003).
- ¹⁹⁸ D. M. Basko, I. L. Aleiner, B. L. Altshuler, Annals of Physics, **321**, 1126 (2006).
- ¹⁹⁹ I. V. Gornyi, A. D. Mirlin, and D. G. Polyakov, Phys. Rev. Lett. **95**, 206603 (2005).
- ²⁰⁰ L. Fleishman, P.W. Anderson, Phys. Rev. **B 21**, 2366 (1980).
- ²⁰¹ V. Oganesyan, D.A. Huse, Phys. Rev. **B 75**, 155111(2007).
- ²⁰² A. Pal, D.A. Huse, Phys. Rev. **B 82**, 174411 (2010).
- ²⁰³ Here are quotes by Konstantin B. Efetov, as cited from my memory: *If I encounter an interesting problem, I first try to solve it myself* (1992). *It is much more difficult to derive and discover something for the first time yourself than to follow others. Nowadays, that does not necessarily give you more credit in the society, but it will be much more satisfying in the end* (1996). *Somehow the best physics always emerges, when a great physicist just had some fun* (2006).